Proc. NIPR Symp. Antarct. Meteorites, **2**, 75–108, 1989

PETROCHEMICAL STUDY OF THE YAMATO-691 ENSTATITE CHONDRITE (E3) III: DESCRIPTIONS AND MINERAL COMPOSITIONS OF CHONDRULES

Yukio IKEDA

Department of Earth Sciences, Faculty of Science, Ibaraki University, 1–1, Bunkyo 2-chome, Mito 310

Abstract: The Yamato-691 enstatite chondrite includes abundant chondrules of various textural types. Among them radial-Px type is the most predominant and the largest. Barred-Ol-Px type and porphyritic to granular types are common. Cryptocrystalline chondrules are small and transparent-SiO_2 chondrules are rare. The constituents of these chondrules are forsterite, enstatite, bronzite, diopside, spinel, plagioclase, silica mineral and/or glass with small amounts of metals and sulfides. Generalized crystallization sequence of chondrules is olivine, low-Ca pyroxene, high-Ca pyroxene, spinel, plagioclase, silica minerals, and glass, in the order. MgO/(MgO+FeO) molar ratios of olivine in barred-Ol-Px, prophyritic to granular, and radial-Px chondrules are 0.92–0.99, 0.98–0.99, and 0.96–0.99, respectively. Ferroan olivines in barred-Ol-Px chondrules experienced various degrees of reduction after solidification, indicating that they were formed under oxidizing conditions and later they were reduced by reaction with a reducing gas. On the other hand, FeO-bearing olivine in radial-Px chondrules seems to be relict and reacted with the chondrule melts at high-temperatures to produce dusty olivine. MgO/(MgO+FeO) molar ratios of pyroxenes are 0.81–0.99 for barred-Ol-Px chondrules, 0.96–1.00 for porphyritic to granular chondrules, and 0.74–1.00 for radial-Px chondrules. Al_2O_3 of high-Ca pyroxene ranges widely from 2 up to 18 wt% and is more than that of coexisting low-Ca pyroxene. The Al_2O_3 content of pyroxene increases with decreasing temperature during crystallization. Low-Ca pyroxene in barred-Ol-Px chondrules is orthopyroxene and richer in Al_2O_3 (1–14 wt%) than that in porphyritic to granular and radial-Px chondrules (less than 1 wt%), which crystallized originally as protoenstatite. Pure albite in peripheral portions of some chondrules may have been formed from aluminous diopside by introduction of alkalies from the ambient reducing gas. Magnesian nature of spinel in some chondrules is due to diffusional exchange of Mg and Fe in a reducing gas. Silica minerals which were precursors of transparent-SiO_2 chondrules might have been produced by oxidation of metallic silicon in Fe-metals and/or fractional condensation of a reducing nebular gas.

1. Introduction

The Yamato-691 enstatite chondrite includes abundant chondrules which show various kinds of texture. Outlines of chondrules are very sharp under a microscope and clean glasses are observed in some chondrules. In addition to these, MgO/(MgO+FeO) molar ratios (hereafter, *mg* values) of pyroxenes in chondrules range from 0.74 to nearly 1.00. These facts indicate that the Y-691 chondrite has not suffered from remarkable thermal metamorphism after formation of the chondrite.

Therefore, chondrules provide good informations on chondrules for a study of mineralogy, crystallization and origin of chondrules in enstatite chondrites.

Petrology of the Y-691 chondrite was reported by OKADA (1975) and OKADA *et al.* (1975). In this paper, detailed description, mineralogy, and crystallization sequence of Y-691 chondrules, and the origin will be discussed. The companion papers by the author (IKEDA, 1988a, b, 1989) deal with major element chemical compositions of chondrules and inclusions in Y-691, descriptions and mineral compositions of unusual silicate-inclusions, and mineral chemistry of opaque-mineral nodules, respectively.

2. Analytical Methods

Chemical compositions of silicates and oxides were obtained using a fixed focussed beam of an electron-probe microanalyser (EPMA, JEOL Superprobe 733, accelerating voltage 15 kV, sample current 3 to 5 nA). Correction method by BENCE and ALBEE (1968) was used for silicates, oxides and glasses. Sulfides and metals were corrected by standard ZAF method.

3. General Descriptions

The Y-691 chondrite consists of unusual silicate-inclusions, chondrules, opaque-mineral nodules, mineral fragments and matrix. In this paper, the term "chondrule" includes droplet chondrules, chondrule fragments, and lithic fragments. Silicate mineral fragments are defined to be single crystals larger than micron size with or without minor other phases, and matrix is interstice-filling materials finer than micron size.

Many kinds of chondrules occur in Y-691, the main type being radial-pyroxene (Px) chondrules. Porphyritic to granular and barred-olivine (Ol)-Px chondrules are common, and minor types include spherulitic and massive cryptocrystalline, and transparent-SiO_2 chondrules. The transparent-SiO_2 chondrules are small spherical ones consisting mainly of silica which are transparent under a microscope. The size frequency of each textural type of chondrules is shown in Fig. 1. Radial-Px type is the largest, porphyritic to granular and barred-Ol-Px types are intermediate, and most cryptocrystalline chondrules are smaller than 0.3 mm. All transparent-SiO_2 chondrules which are not shown in Fig. 1 are smaller than 0.2 mm across.

4. Barred-Ol-Px Chondrules

Barred-Ol-Px chondrules consist mainly of barred pyroxene with variable amounts of barred or blebby olivine. They are mostly holocrystalline. The bulk chemical compositions of this type are characterized by high Al_2O_3 (more than 3 wt%) and high CaO (more than 2.5 wt%) contents in comparison to other textural types, and the *mg* values range from 0.85 to 0.98 (IKEDA, 1988a). Chemical compositions of the constituent minerals and glasses of this type are tabulated in Appendix I, and the *mg* values and the compositional range in Al_2O_3 of pyroxene are

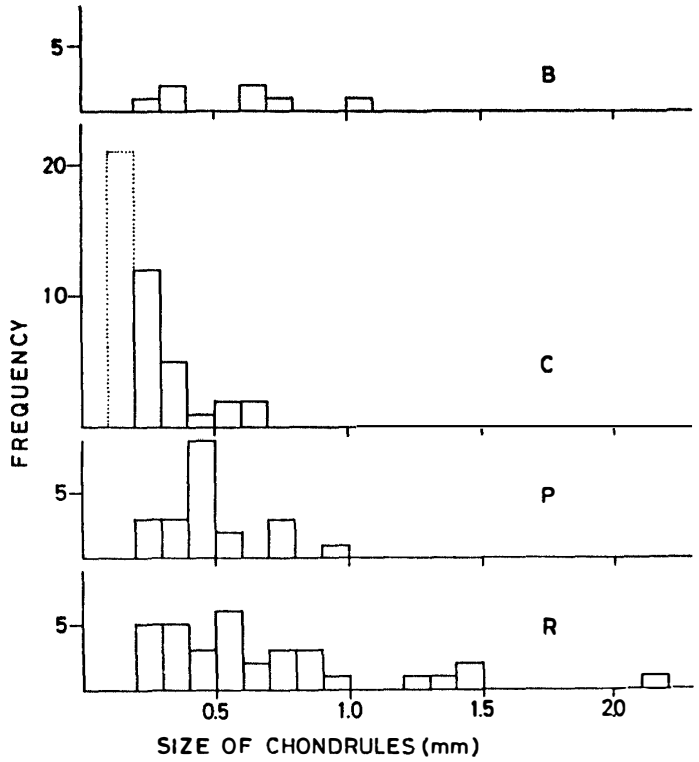

Fig. 1. Size and frequency of each textural type of Y-691 chondrules. Size is arithmetic mean of length and width of chondrules, and the chondrules larger than 0.2 mm are shown. The abbreviation, B, C, P, and R are barred-Ol-Px, cryptocrystalline, porphyritic to granular, and radial-Px chondrules, respectively. Cryptocrystalline chondrules show a peak at a size smaller than 0.2 mm. Transparent-SiO_2 chondrules are smaller than 0.2 mm, and they are not shown here.

shown in Table 1.

4.1. Sp-bearing and En-free barred-Ol-Px chondrules

Chondrule No. 310 (Fig. 2a) is a unique barred-Ol-Px chondrule which lacks enstatite. It consists mainly of olivine, diopside, and minor spinel. Olivine and diopside occur as bars, and the width is several microns for olivine and a few microns for diopside. Olivine is homogeneous in chemical composition. Diopside contains Al_2O_3 up to 13.6 wt% and the TiO_2 and Cr_2O_3 increase up to 1.47 wt% and 1.41 wt%, respectively with increasing Al_2O_3 (Appendix I). Spinel occurs as small euhedral to subhedral grains, about a few to several microns across, in association with aluminous diopside (Fig. 2b) and has high FeO (about 8 wt%) and Cr_2O_3 (about 17 wt%) contents.

4.2. Sp-bearing barred-Ol-Px chondrules

This type consists mainly of olivine, enstatite, diopside, and spinel. The main constituent is enstatite occurring as bars which are several to a few tens of microns in width. The enstatite is orthopyroxene. Spinel occurs as small rounded or anhedral grains, less than a few tens of microns across, near or in aluminous pyroxene.

In chondrule No. 264 (Fig. 3a), olivine occurs as bars narrower than 10 μm, and

Table 1. Mg/(MgO+FeO) molar ratios of olivine (Ol), low-Ca pyroxene (En), high-Ca pyroxene (Di), and spinel (Sp), and compositional range in Al_2O_3 wt% of low-Ca pyroxenes.

Chondrule number	MgO/(MgO+FeO) ratios				Al_2O_3 wt%	
	Ol	En	Di	Sp	En	Di
Barred-Ol-Px chondrules						
310	0.92–0.93		0.90–0.93	0.84		5–14
264	0.94–0.96	0.95–0.96	0.93–0.96	0.99–1.00	2–14	4–18
176	0.96–0.97	0.97–0.98	0.96–0.97	0.99	2–9	2–13
266	0.96–0.97	0.95–0.96	0.95–0.96	0.99	2–7	5–14
267	0.98–0.99	0.98–0.99	0.97–0.98		7–9	8–10
259	0.95–0.96	0.93–0.95	0.92–0.94		4–8	8–10
120	0.96–0.97	0.96–0.97	0.96		2–5	4–8
169	0.93	0.81–0.88			1–5	
Porphyritic to granular chondrules						
159	0.98–0.99	0.99			1.0	
110	0.99	0.98–0.99			0.0–0.3	
149	0.99	0.99	0.96–0.99		0.3–0.5	3–9
109	0.99	0.99			0.2–0.7	
115	0.99	0.98–0.99			0.2–0.3	
117	0.98–0.99	0.98	0.99		0.1–0.4	10–13
158		0.99–1.00			0.5–0.9	
244	0.99	0.99	0.98–0.99		0.4–1.0	3–5
238		0.99	0.99–1.00		0.2–0.7	3–4
Radial-Px chondrules						
100	0.96–0.98	0.95–0.97	0.92		0.2	6
307	0.97–0.99	0.97–0.98			0.1–0.6	
101		0.97	0.96		0.2–0.3	2
127		0.99	0.98		0.2–0.4	6
161		0.97–0.98	0.96–0.97		0.3–0.4	2–3
116		0.93–0.94			0.1–0.2	
128		0.98–0.99			0.1–0.2	
175		0.99			0.1–0.3	
268		0.99–1.00	1.00		0.2–0.4	5
154		0.74–0.91			0.1–0.5	

some portions of olivine bars have been changed into fine-grained aggregates of Mg-silicates and Fe-metal, showing a striped pattern (decomposed-olivine, hereafter) (Fig. 3b). Enstatite contains Al_2O_3 up to 14 wt%, and Al-poor ($Al_2O_3 < 5$ wt%) enstatite is slightly more magnesian ($mg = 0.95$–0.97) in comparison to Al-rich ($Al_2O_3 > 5$ wt%) enstatite ($mg = 0.95$–0.96). Diopside also shows a wide continuous range in Al_2O_3 up to 18 wt%. The *mg* value (0.92–0.96) of Al-rich ($Al_2O_3 > 10$ wt%) is slightly smaller than that (0.93–0.97) of Al-poor ($Al_2O_3 < 10$ wt%) diopside. Spinel is extremely magnesian and the *mg* value is larger than those of the coexisting pyroxenes. Albite occurs in the peripheral parts of the chondrule.

In chondrule No. 176, olivine occurs as small blebby grains a few to ten microns across, and sometimes it is included in enstatite and diopside. The blebs of olivine sometimes arrange in a string of beads. Enstatite is more magnesian than diopside. Diopside shows euhedral to subhedral forms, elongating parallel to the

Fig. 2a. Photomicrograph (crossed Nicols) of No. 310. Width is 570 μm.

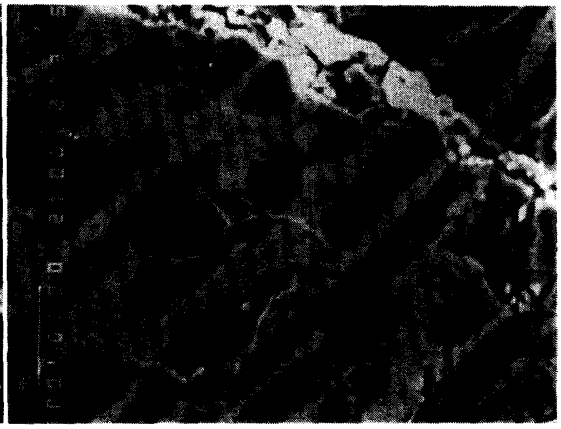

Fig. 2b. BSE image of No. 310. Olivine (Ol) and diopside (Di) occur as bars. Several spinel grains (Sp) occur associated with fassaitic diopside ($Al_2O_3 > 10$ wt%) (Fa). Width is 56 μm.

Fig. 3a. Photomicrograph (open Nicols) of No. 264. Width is 570 μm.

Fig. 3b. BSE image of No. 264. Enstatite (En) and diopside (Di and Fa) occur as larger bars and decomposed olivine (dOl) occurs as smaller bars. Note striped patterns of decomposed-olivine. Width is 110 μm.

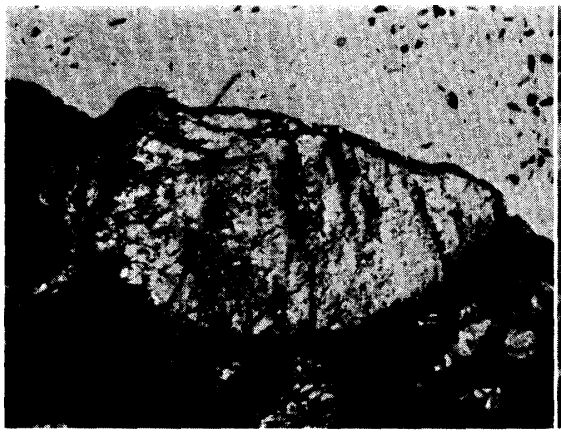

Fig. 4a. Photomicrograph (open Nicols) of No. 266. Width is 1.15 mm.

Fig. 4b. BSE image of No. 266. It is observed in the central portion of the image that albite (Ab) includes Al-poor diopside (Di). Width is 52 μm.

Fig. 5. Photomicrograph (crossed Nicols) of No. 267. Width is 1.15 mm.

Fig. 6. Photomicrograph (crossed Nicols) of No. 120. Width is 570 μm.

Fig. 7a. Photomicrograph (open Nicols) of No. 169. Width is 2.3 mm.

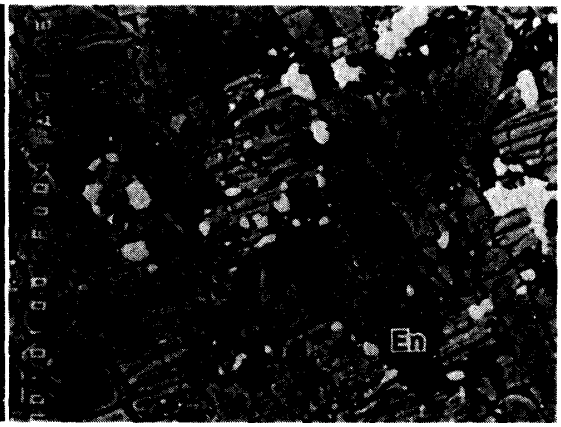

Fig. 7b. BSE image of No. 169. Bronzite (Br) and decomposed-olivine (dOl) occur as long and short bars, respectively. Enstatite (En) occurs as pseudomorph after olivine. White minerals are Fe-metal. Note striped patterns of decomposed-olivine. Width is 110 μm.

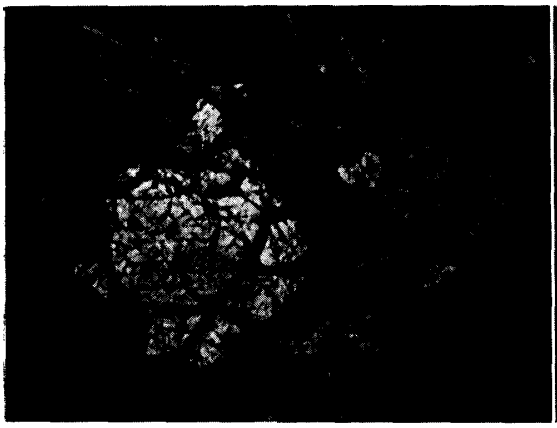

Fig. 8. Photomicrograph (crossed Nicols) of No. 159. Width is 1.15 mm.

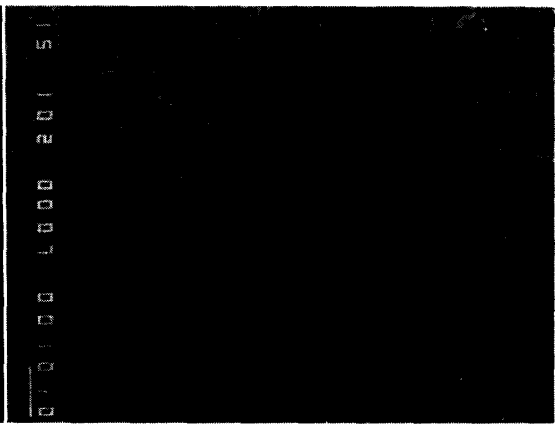

Fig. 9. BSE image of No. 149. Note decomposition of aluminous diopside into plagioclase (Pl) and Al-poor diopside (Di). Width is 110 μm.

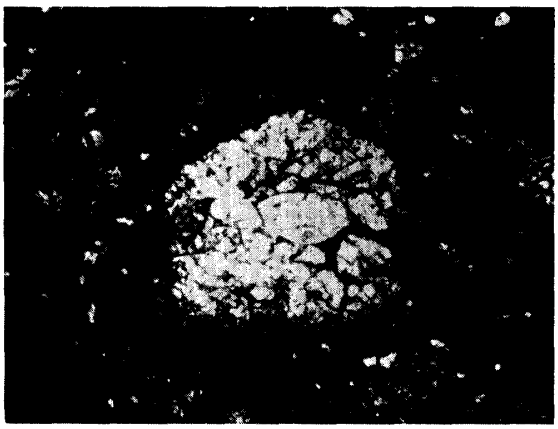

Fig. 10a. Photomicrograph (open Nicols) of No. 109. Width is 2.3 mm.

Fig. 10b. BSE image of No. 109. Note a shark-teeth structure of diopside (Di) between glass (Gl) and enstatite (En). Width is 56 μm.

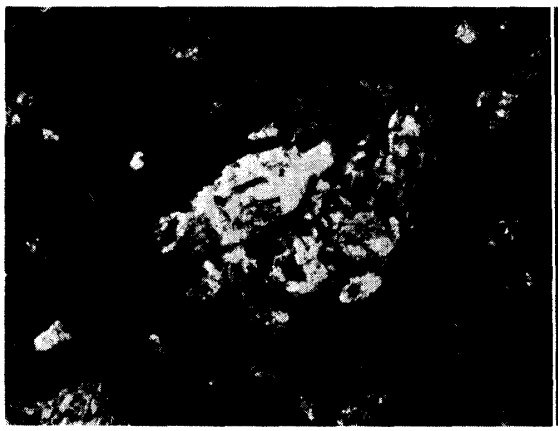

Fig. 11a. Photomicrograph (crossed Nicols) of No. 117. Width is 1.15 mm.

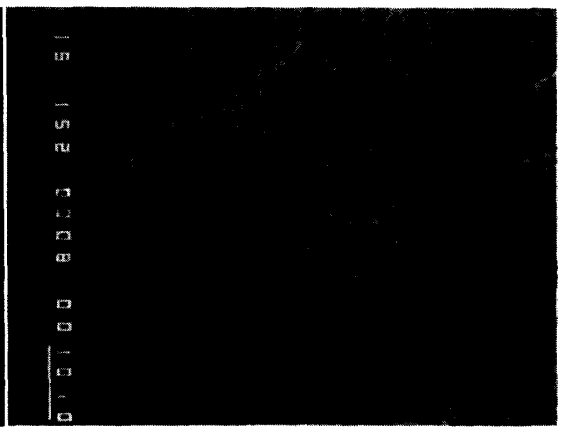

Fig. 11b. BSE image of No. 117. Note plagioclase (Pl) in mesostasis and euhedral fassaitic diopside (Fa) at the rim of large enstatite (En). Width is 73 μm.

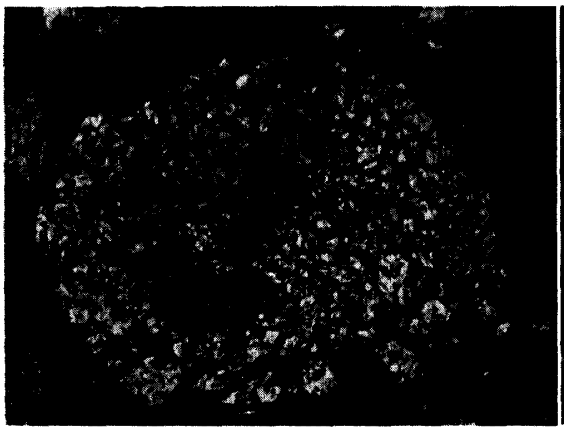

Fig. 12a. Photomicrograph (open Nicols) of No. 244. Width is 570 μm.

Fig. 12b. BSE image of No. 244. Diopside (Di) occurs at the rim of enstatite (En) setting in glass (Gl). Width is 56 μm.

Fig. 13a. Photomicrograph (open Nicols) of No. 238. Width is 570 mm.

Fig. 13b. BSE image of No. 238. Note euhedral diopside grains (Di) and a silica mineral (Si) setting in glass (Gl). Width is 73 μm.

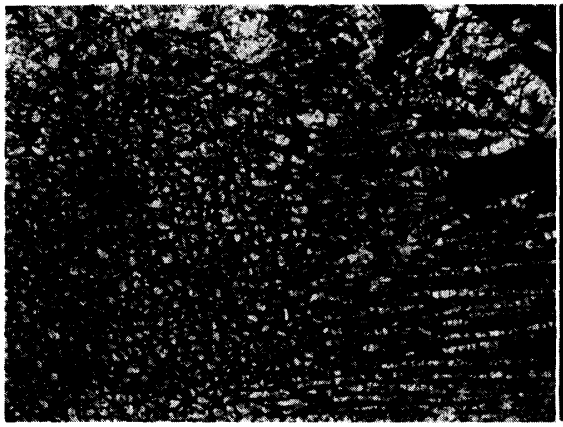

Fig. 14a. Photomicrograph (open Nicols) of No. 100. Width is 2.3 mm.

Fig. 14b. BSE image of dusty olivine in No. 100. Note tiny metallic grains (white spots) in olivine (gray). Width is 56 μm.

Fig. 14c. BSE image of No. 100. Note rounded silica-mineral grains (Si) and diopside (Di) occurring in mesostasis glass (Gl). Width is 110 μm.

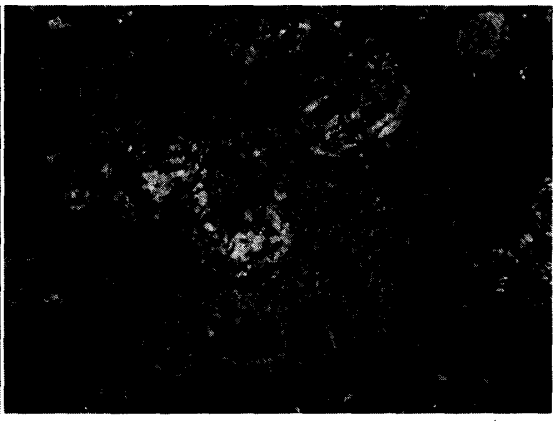

Fig. 15. Photomicrograph (open Nicols) of No. 307. An aggregate of enstatite and Fe-metal occurs at the upper-right portion of the chondrule. Width is 1.15 mm.

Fig. 16. Photomicrograph (open Nicols) of No. 127. Width is 2.3 mm.

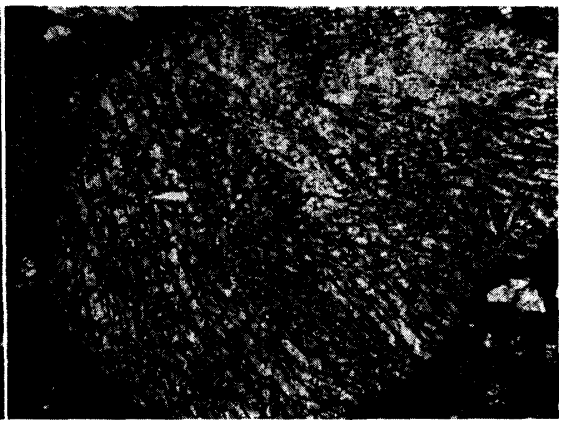

Fig. 17a. Photomicrograph (open Nicols) of No. 161. Width is 1.15 mm.

Fig. 17b. BSE image of No. 161. Note a ladder structure consisting of diopside (Di) and silica mineral (Si). Width is 56 μm.

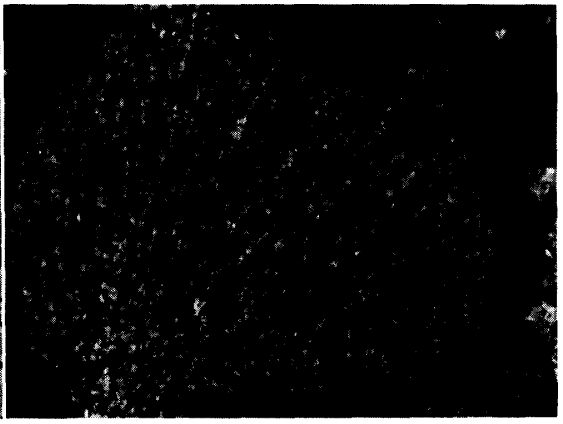

Fig. 18. Photomicrograph (open Nicols) of No. 116. Width is 570 μm.

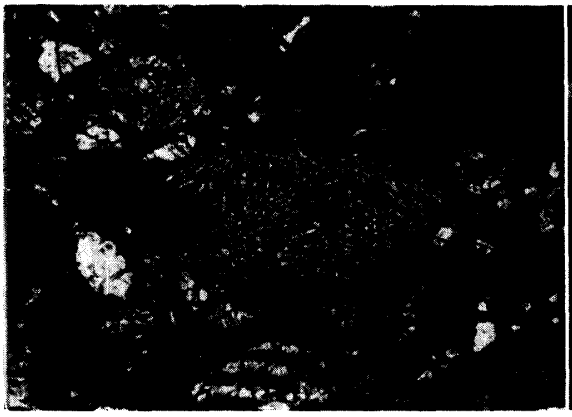

Fig. 19. Photomicrograph (open Nicols) of No. 175. Width is 1.15 mm.

Fig. 20. Photomicrograph (open Nicols) of No. 268. Width is 1.15 mm.

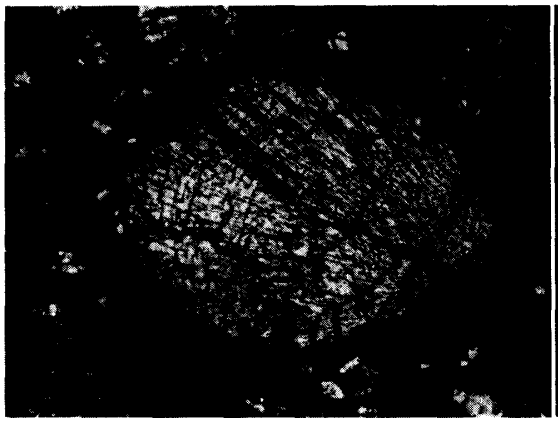

Fig. 21a. Photomicrograph (crossed Nicols) of No. 154. Width is 1.15 mm.

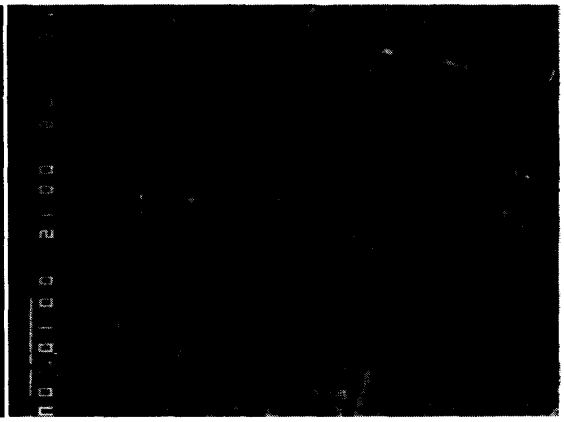

Fig. 21b. BSE image of No. 154. Note a normal zoning of bronzite (Br); dark and light portions are magnesian and ferroan pyroxenes, respectively. Width is 56 μm.

Fig. 22. Photomicrograph (crossed Nicols) of No. 171. Width is 570 μm.

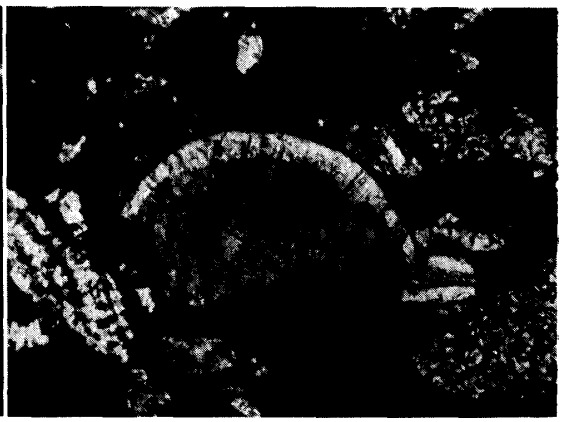

Fig. 23. Photomicrograph (crossed Nicols) of No. 131. Width is 570 μm.

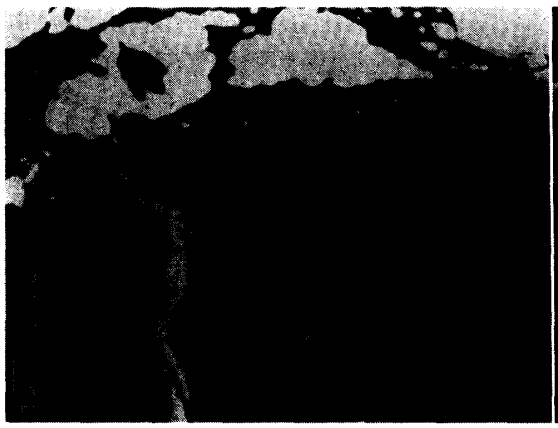

Fig. 24. BSE image of No. 151. Note rounded silica-mineral grains (Si) at the rim of chondrule. Width is 56 μm.

Fig. 25a. Photomicrograph (open Nicols) of No. 150. Width is 570 μm.

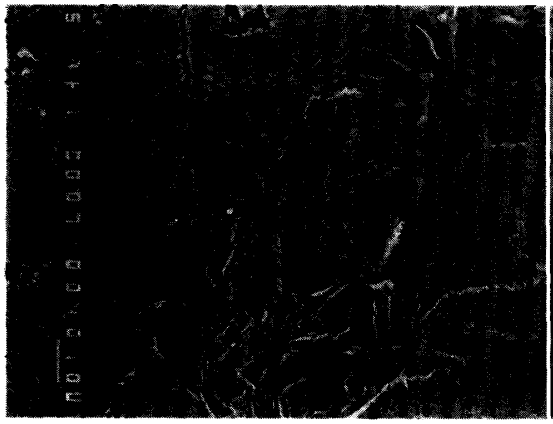

Fig. 25b. BSE image of No. 150. Note rounded silica-mineral grains (Si) setting in cryptocrystalline groundmass. Width is 130 μm.

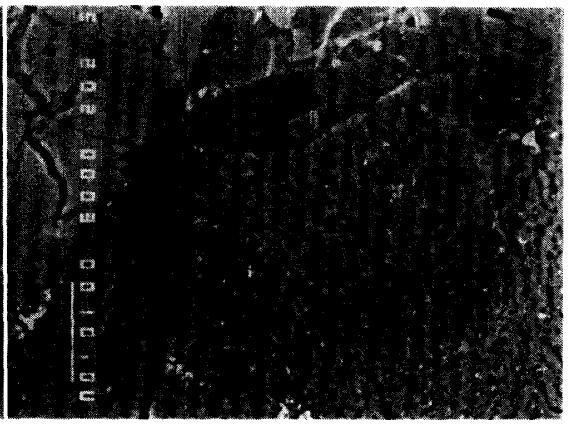

Fig. 26. BSE image of No. 138. Note a silica-mineral mantle (Si) and a cryptocrystalline core. Width is 56 μm.

Fig. 27a. Photomicrograph (open Nicols) of No. 219. Width is 570 μm.

Fig. 27b. BSE image of No. 219. Note phenocrystic silica-mineral grains (Si) and cryptocrystalline groundmass showing a dendritic texture of pyroxene. Width is 56 μm.

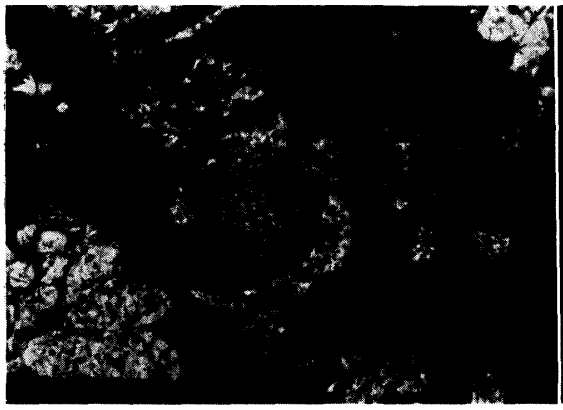

Fig. 28. Photomicrograph (open Nicols) of No. 215. The cryptocrystalline chondrule is completely surrounded by silica-mineral mantle, the width of the mantle being 12–36 μm. Width is 570 μm.

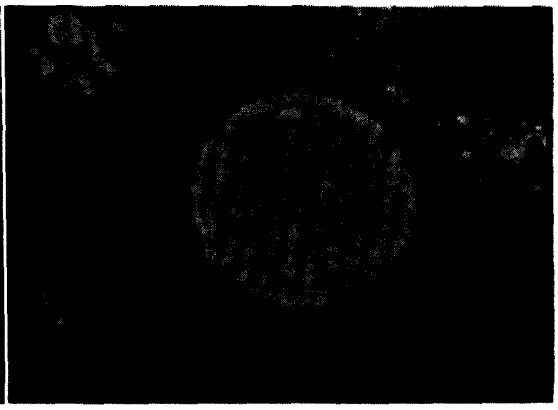

Fig. 29. Photomicrograph (open Nicols) of No. 142. Width is 290 μm.

enstatite bars. Spinel is more magnesian than the coexisting other phases. Small amounts of troilite and Fe-metal occur.

In chondrule No. 266 (Fig. 4a), olivine shows rounded outlines included in enstatite, the diameter is a few to ten microns. Diopside shows euhedral to subhedral forms parallel to the enstatite bars. Spinel is the most magnesian in the chondrule. Albite occurs as pseudomorphs after aluminous diopside and Al-poor diopside is included in the albite (Fig. 4b). Small amounts of troilite and Fe-metal occur.

4.3. Sp-free barred-Ol-Px chondrules

This type consists mainly of olivine, enstatite, and diopside, the main phase being enstatite of orthopyroxene. The texture is similar to that of Sp-bearing barred-Ol-Px chondrules.

In chondrule No. 267 (Fig. 5), olivine occurs as thin short bars or a string of blebs, and the width or diameter is less than ten microns. Diopside shows subhedral forms and the size is similar to that of olivine. Small amount of troilite and Fe-metal occur.

In chondrule No. 259, olivine is fine-grained (several microns across) and ovoid in shape, sometimes arranging like a string of beads. Diopside is fine-grained, several microns across. In chondrule No. 120 (Fig. 6), olivine occurs as blebs and the size is several to ten microns across. Diopside shows euhedral to subhedral forms, the size being several to a few tens of microns across.

4.4. Bronzite-bearing barred-Ol-Px chondrules

Chondrule No. 169 (Fig. 7a) shows an atypical barred-Ol-Px texture, consisting of decomposed-olivine, bronzite, enstatite, plagioclase, troilite and Fe-metal. The decomposed-olivine consists of Mg-silicates, olivine, and Fe-metal, showing a striped pattern (Fig. 7b). It may have been originally ferroan olivine occurring as blebs or short bars. Bronzite is predominant in the chondrule and occurs as bars, the width being less than a few tens of microns. There is a weak tendency that the bronzite with smaller *mg* values is higher in CaO content. Enstatite occurs with minor Fe-metal in the central portion of the chondrule as pseudomorphs after olivine bars or blebs, and is secondary enstatite. CaO, FeO, and Al_2O_3 contents of the secondary enstatite are less than 0.11, 0.44, and 0.19, respectively. In contrast, those of primary bronzite are more than 0.87, 8.1, 0.84, respectively. Plagioclase occurs in interstitial spaces among bronzite and/or decomposed-olivine bars. The composition is $An_{72.5}Ab_{27}$ to $An_{67.5}Ab_{32}$.

5. Porphyritic to Granular Chondrules

Porphyritic Ol-Px or Px chondrules and granular chondrules are common in Y-691. The modal ratios of olivine to pyroxene are smaller than barred-Ol-Px chondrules and larger than those of radial-Px chondrules. Most chondrules belonging to this type include clean or devitrified glass or mesostasis in the groundmass. Metals and sulfides sometimes occur in small amounts. Chondrules of this type are magnesian in bulk compositions in comparison to those of barred-Ol-Px type and the *mg*

value is larger than 0.95 (IKEDA, 1988a). Chemical compositions of the constituents of this type are tabulated in Appendix II, and the *mg* values and the compositional range in Al_2O_3 of pyroxene are shown in Table 1.

5.1. Porphyritic Ol-Px chondrules

This type consists mainly of olivine and enstatite with minor mesostasis. The olivine and enstatite occur as large phenocrystic crystals showing euhedral or subhedral forms. Enstatite in some chondrules of this type shows remarkable polysynthetic twinning, indicating that it inverted from protoenstatite to clinoenstatite. Mesostasis consists of enstatite, diopside, plagioclase, and/or glass with or without sulfide and metal.

In chondrule No. 159 (Fig. 8), phenocrystic olivine shows a weak normal zoning with the *mg* ranging from 0.99 to 0.98. Fe-metal, troilite and niningerite occur in small amounts in the mesostasis. In chondrule No. 110, enstatite occurs as large phenocrystic grains and as small grains in mesostasis. The former (mg=0.98–0.99) is more magnesian than the latter (mg=0.98). Small amounts of Fe-metal and troilite occur in the mesostasis. In chondrule No. 149, mesostasis consists of diopside and plagioclase. Al-rich (about 9 wt%) diopside occurs as a primary mineral, but Al-poor (about 3 wt%) diopside occurs in fine-grained aggregates with plagioclase after pseudomorph of Al-rich diopside (Fig. 9). The Al-poor diopside may be secondary one. The secondary Al-poor diopside (mg=0.99) is more magnesian than the primary Al-rich diopside (mg=0.96). Plagioclase is $An_{48}Ab_{50}Or_2$.

5.2. Ol-bearing porphyritic Px chondrules

This type consists mainly of olivine, phenocrystic enstatite, and mesostasis. The phenocrystic enstatite includes small rounded or subhedral olivine grains. Mesostasis consists of diopside, plagioclase, and/or glass with or without minor sulfide and metal.

In chondrule No. 109 (Fig. 10a), the mesostasis consists of clean glass and diopside, and alkali content of the glass is high (Na_2O+K_2O=10–11 wt%). Diopside occurs between enstatite and mesostasis glass, showing a shark-teeth texture (Fig. 10b). Troilite and minor Fe-metal occur in the mesostasis as small globules about 20–30 μm across. In chondrule No 115, the mesostasis is clean glass having high contents of CaO and Al_2O_3 ($CaO+Al_2O_3$=25–30 wt%). In chondrule No. 117 (Fig. 11a), diopside and plagioclase occur in mesostasis (Fig. 11b). The former is aluminous diopside, containing high Al_2O_3 (Al_2O_3=10–13 wt%) and TiO_2 (about 1.6 wt%). The composition of plagioclase is $An_{84}Ab_{16}$ to $An_{79}Ab_{20}$. Troilite and Fe-metal occur as small globules about 20 μm across in the chondrule.

5.3. Equigranular chondrules

This type consists mainly of magnesian enstatite with the *mg* of 0.98–0.99 and minor mesostasis, and olivine is absent or minor.

In chondrule No. 244 (Fig. 12a), olivine occurs as corroded grains. Diopside occurs in mesostasis glass, showing euhedral forms (Fig. 12b). In chondrule No. 158, the groundmass is clean glass and the composition is albitic ($An_1Ab_{95}Or_4$). Troilite

and Fe-metal occur as small grains, and sometimes the former is included by the latter.

5.4. Microporphyritic chondrules

Chondrule No. 238 (Fig. 13a) consists of enstatite, diopside, silica mineral and glass with a small amount of Fe-metal. Enstatite shows a euhedral form, the size being ten to one hundred of microns across. Diopside occurs as rims of enstatite and as euhedral grains in mesostasis glass (Fig. 13b). A silica mineral shows subhedral to euhedral forms in glass, and seems to be the last phase which crystallized from the residual melt of the chondrule. The mesostasis includes clean glass and the chemical composition corresponds nearly to alkali feldspar. The glass contains a high content of K_2O (about 3 wt%), and the K/Na ratio is the highest among all glasses in Y-691.

6. Radial-Pyroxene Chondrules

Radial-Px chondrules are the main type in Y-691. Sometimes they include olivine crystals which show subhedral outlines with corrosion textures. A silica mineral occurs commonly in mesostasis. Metals and sulfides are included in small amounts. The bulk chemical compositions of radial-Px chondrules range in the *mg* values from 0.84 to 0.99 (IKEDA, 1988a), Chemical compositions of the constituents of this type are tabulated in Appendix II, and the *mg* values and the compositional range in Al_2O_3 of pyroxene are shown in Table 1.

6.1. Ol-bearing radial-Px chondrules

This type consists mainly of olivine, enstatite, and mesostasis with small amounts of sulfide and Fe-metal. The main constituent is enstatite, and olivine is minor. The mesostasis includes diopside, silica mineral, and/or glass. Olivine occurs as large grains up to 200 μm, showing subhedral or corroded outlines. It is observed under a microscope that the interiors of some large olivine grains become dusty although the peripheral portions remain fresh olivine which is homogeneous in chemical composition. BSE images reveal that the dusty olivine includes many tiny grains of Fe-metal with or without Mg-silicates. The size of Fe-metal is smaller than one micron (Fig. 14b). The texture is quite different from that of decomposed-olivines showing striped patterns (Figs. 3b and 7b), which occur in barred-Ol-Px chondrules.

In chondrule No. 100 (Fig. 14a), diopside and a silica mineral occur in mesostasis together with glass (Fig. 14c). Diopside shows euhedral to subhedral forms and has high contents of Cr_2O_3 (3–4 wt%), TiO_2 (about 1 wt%) and Al_2O_3 (about 6 wt%). The silica mineral shows a rounded form and occupies nearly a half area of the mesostasis (Fig. 14c). In chondrule No. 307 (Fig. 15), an aggregate, about 50 μm across, occurs at the rim, consisting of FeO-free enstatite and rounded Fe-metal grains up to about a few tens of microns. It seems to be secondary enstatite because it occurs after the pseudomorph of an olivine grain. CaO, FeO, and Al_2O_3 contents of the secondary enstatite are less than 0.1, 1.0, and 0.1, respectively, which are lower in comparison to those of primary ones. Troilite and Fe-metal occur in small amounts and a large troilite grain, about 50×100 μm, includes thin daubreelite lamellae.

6.2. Ol-free excentroradial-Px chondrules

Chondrules Nos. 101, 127 (Fig. 16), and 161 (Fig. 17a) consist mainly of enstatite and mesostasis with small amounts of sulfide and Fe-metal. The mesostasis includes diopside, silica mineral and/or glass.

In chondrule No. 127 (Fig. 16), diopside occurs in the mesostasis and the TiO_2 (1.87 wt%) and Al_2O_3 (6.4 wt%) contents are high. In chondrule No. 161 (Fig. 17a), diopside and silica mineral in the mesostasis show a ladder texture (Fig. 17b), which is constructed by parallel elongated crystals of diopside and silica mineral. Interstitial glass is nearly albitic ($An_1An_{88}Or_{11}$) in chemical composition.

6.3. Opaque-mineral-rich radial-Px chondrules

Some radial-Px chondrules include opaque minerals in fairly large amounts. The opaque minerals are mainly Fe-metal and troilite, and the modal amounts seem to be several percents. The mesostasis includes silica mineral, albite, and/or glass.

The *mg* value of enstatite in chondrule No. 116 (Fig. 18), is relatively low, and the Cr_2O_3 content is high (1.1–1.3 wt%). In chondrule No. 128, the mesostasis includes albite which is close to pure albite in chemical composition.

6.4. Multi-centric radial-Px and centroradial-Px chondrules

Chondrule No. 175 shows a multi-centric radial-Px texture (Fig. 19), consisting of enstatite and mesostasis. The mesostasis inlcudes a silica mineral.

Chondrule No. 268 shows a coarse-grained centroradial-Px texture (Fig. 20). It consists of enstatite and mesostasis. Enstatite sometimes includes many small blebs of a silica mineral. The mesostasis consists of diopside, silica mineral, and glass. The diopside occurs as rim of enstatite and as euhedral needle crystals in mesostasis glass. The TiO_2 (1.2–1.5 wt%) and Al_2O_3 (4.9–5.1 wt%) contents are relatively high. Chemical composition of the glass is nearly albitic ($An_1Ab_{97}Or_2$).

6.5. Bronzite-bearing radial-Px chondrules

Chondrule No. 154 (Fig. 21a) consists mainly of bronzite. Small amounts of Fe-metal and troilite are included in bronzite, but no interstitial material is observed. A silica mineral is adhered partly at the edge of the chondrule, which seems to have attached from outside of the chondrule. The bronzite ranges in the *mg* value from 0.71 to 0.91, and shows a normal zoning from Mg-rich core to F-rich rim in the direction perpendicular to elongation (Fig. 21b). The Cr_2O_3 content increases from 1.1 to 2.1 wt% with increasing FeO.

7. Cryptocrystalline and Transparent-SiO_2 Chondrules

Cryptocrystalline type includes two subtypes: spherulitic and massive. The former is generally small, ranging from several tens to about 200 μm across. Most of them show circular or ellipsoidal outlines. The latter shows no specific texture and the size ranges from smaller than 100 μm to 0.7 mm across. Intermediate type between the two subtypes is observed. Sometimes, cryptocrystalline chondrules include small needles or laths of a silica mineral in a small amount. Some crypto-

crystalline chondrules show a concentric structure with a fine-grained mantle and a cryptocrystalline core.

Transparent-SiO_2 chondrules are smaller than about 150 μm in diameter and show always spherical outlines. They are nearly pure SiO_2 in chemical composition.

Chemical compositions of the constituents in cryptocrystalline and transparent-SiO_2 chondrules are tabulated in Appendix III.

7.1. Spherulitic cryptocrystalline chondrules

Chondrule No. 171 (Fig. 22) shows a typical spherulitic texture. BSE images show that it consists of fine-grained radial silicates (probably low-Ca pyroxene) and interstice-filling materials with many small grains of Fe-metal. Chondrule No. 131 shows a concentric structure (Fig. 23). The outer zone, about 60 μm in width, consists of very fine-grained low-Ca pyroxene, and the interior is cryptocrystalline material. BSE images show that the interior consists of fine-grained olivine and interstice-filling silicates with minor metallic phases. Chondrule No. 151 shows partly spherulitic texture. Small rounded grains of a silica mineral occur at the rim of the chondrule (Fig. 24), which seems to have crystallized from the rim towards the interior. Chondrule No. 150 shows a spherulitic texture (Fig. 25a), including small silica-mineral crystals. The silica mineral is several tens of microns in size, and seems to have crystallized from the chondrule melt as microphenocrysts. Some silica mineral grains show euhedral forms and others rounded outlines (Fig. 25b).

7.2. Massive cryptocrystalline chondrules

Chondrule No. 138 is surrounded by silica-mineral crystals and the interior is dark and massive. BSE images (Fig. 26) reveal that the dark massive interior consists of fine-grained pyroxene, interstice-filling silicates (probably a silica mineral or silica glass) and small grains of Fe-metal. Silica-mineral crystals surrounding the chondrule seem to have crystallized from the rim towards the interior. Chondrule No. 219 consists of silica mineral crystals and massive groundmass (Fig. 27a). The silica mineral shows a euhedral form, indicating that it crystallized from a melt. BSE images (Fig. 27b) reveal that the massive groundmass consists of dendritic pyroxene and interstice-filling materials (probably a silica mineral or silica glass). Chondrule No. 215 is a cryptocrystalline chondrule surrounded completely by silica-mineral crystals (Fig. 28), and the silica mineral seems to precipitate at the rim of chondrule from the outside after the chondrule solidification.

7.3. Transparent-SiO_2 chondrules

Chondrule No. 142 is a typical transparent-SiO_2 chondrule, showing a spherical outline (Fig. 29). The chemical composition of the chondrule is close to pure SiO_2.

8. Mineralogy

8.1. Olivine

Chondrules in the Y-691 chondrite include a fairly large amount of olivine (about 4%, OKADA, 1975) in comparison to other enstatite chondrites, and olivine occurs

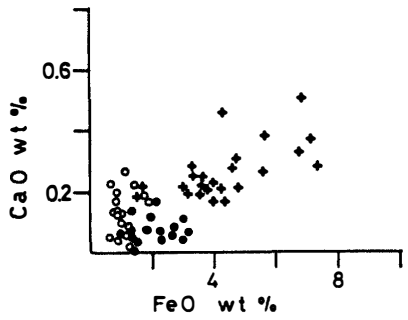

Fig. 30. CaO and FeO wt% of olivines in barred-Ol-Px (cross), porphyritic to granular (open circle), and radial-Px (solid circle) chondrules in Y-691.

commonly in barred-Ol-Px type, sometimes in porphyritic to granular type, and rarely in radial-Px type. Most olivines are the first liquidus phase crystallized from chondrule melts although olivines in some chondrules are a relict mineral. The FeO contents of most olivines in chondrules range from 1 wt% to 8 wt%, and the *mg* values of olivine are 0.92–0.99 for barred-Ol-Px type, 0.98–0.99 for porphyritic to granular type, and 0.96–0.99 for radial-Px type. Most magnesian olivines with the *mg* values larger than 0.95 remain fresh in the chondrules whereas ferroan olivines with those smaller than 0.95 show various degrees of reductive decomposition except for ferroan olivine in chondrule No. 310.

In Fig. 30, chemical compositions of olivines in Y-691 chondrules are shown. The CaO and FeO contents of olivines in barred-Ol-Px type are higher than those in porphyritic to granular and radial-Px types. The CaO content of bulk chondrules of the former type is higher and the *mg* value is lower than those of the latter types (IKEDA, 1988a), suggesting that the chondrule melts which crystallized olivine as a primary liquidus phase were richer in CaO and FeO for the former type, resulting in higher contents of CaO and FeO in olivine of barred-Ol-Px type.

8.2. Low-Ca pyroxene

Low-Ca pyroxene is a predominant phase in most chondrules. They are divided into two groups; primary and secondary. The former is low-Ca pyroxenes which crystallized directly from chondrule melts, and the latter is FeO-free enstatites which were produced after chondrule solidification from ferroan olivines by reaction with an extremely reducing nebular gas (see Section 9.2). The FeO content of primary low-Ca pyroxenes ranges from 0.5 to 17 wt%, although that of secondary enstatites is less than 0.5 wt%. Sometimes the primary enstatites in porphyritic to granular and radial-Px chondrules show polysynthetic twinning, suggesting that they inverted from protoenstatite to clinoenstatite. In contrast, primary enstatite in barred-Ol-Px type shows straight extinction and low birefringence under a microscope, indicating that it is orthopyroxene.

Chemical compositions of primary low-Ca pyroxenes are plotted in Figs. 31, 32 and 33. Figure 31 shows that the primary low-Ca pyroxenes in barred-Ol-Px chondrules except for No. 169 plot in a narrow compositional range; the Ca/(Ca+Mg+Fe) ratios are nearly constant with the values of 3–6% and the *mg* values are 0.99–0.93. Primary low-Ca pyroxenes of barred-Ol-Px chondrule No. 169 are more ferroan and Ca-poor. The CaO content of the bulk chondrule No. 169 is 2.7 wt% which is the lowest among barred-Ol-Px chondrules (IKEDA, 1988a), indicating that the chondrule

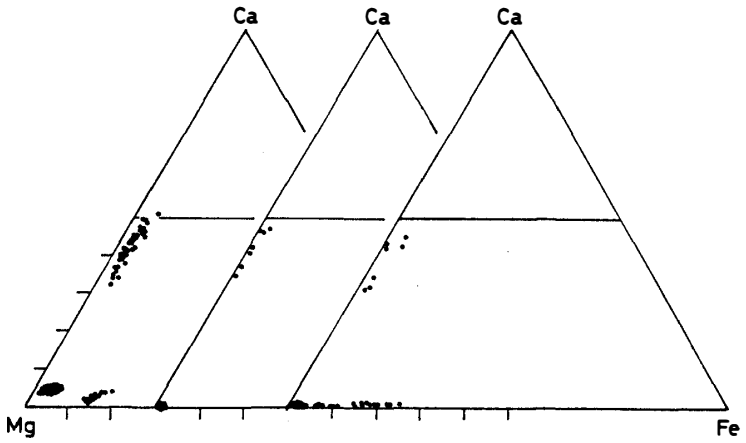

Fig. 31. Chemical composition (atomic ratio) of primary pyroxenes in barred-Ol-Px (left), porphyritic to granular (middle), and radial-Px types (right). Open and solid circles are low-Ca and high-Ca pyroxenes, respectively. In left figure, ferroan low-Ca pyroxenes with the mg value of 0.81–0.88 are bronzite in chondrule No. 169.

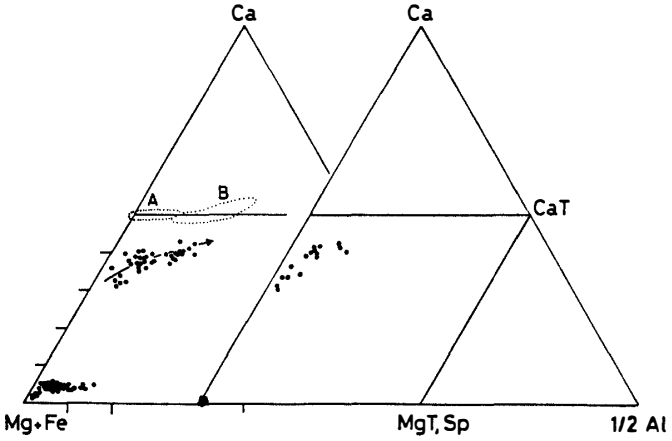

Fig. 32. Chemical composition (atomic ratio) of primary pyroxenes in barred-Ol-Px type (left) and porphyritic to granular and radial-Px types (right). CaT, MbT, and Sp are calcium and magnesium tschermak's molecules and spinel, respectively. Solid circles in left are low-Ca pyroxenes in barred-Ol-Px chondrule No. 169. The compositional ranges of diopside and fassaite in CAI's of types A and B from Allende (Grossman, 1975) are shown by dotted circles denoted by A and B, respectively. The arrow in the left figure shows a crystallization trend of diopside with decreasing temperature.

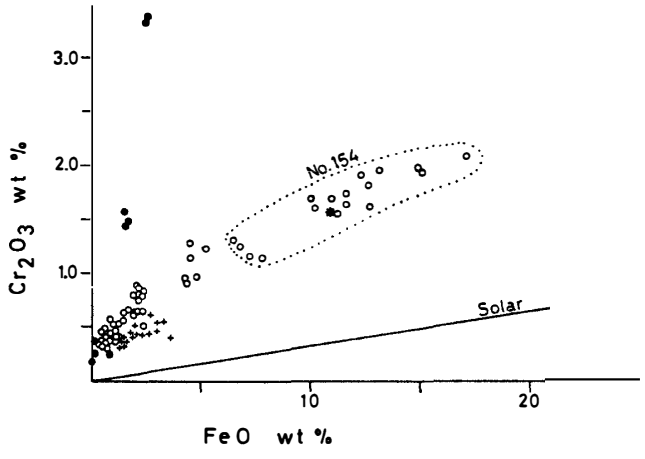

Fig. 33. FeO and Cr_2O_3 contents of primary low-Ca pyroxene (open circles), high-Ca pyroxene (solid circles) and olivine (cross) in radial-Px chondrules.

melt was originally poor in CaO and crystallized CaO-poor pyroxene. The Al_2O_3 contents of primary low-Ca pyroxenes in barred-Ol-Px chondrules are variable (Fig. 32), ranging from 1 to 14 wt%, although that of the ferroan pyroxenes in chondrule No. 169 is relatively low (Fig. 32).

On the other hand, primary low-Ca pyroxenes in porphyritic to granular and radial-Px types are poorer in CaO content than those in barred-Ol-Px type (Fig. 31), and the *mg* values are larger than 0.95, although those of a few radial-Px chondrules (Nos. 116 and 154) range from 0.94 to 0.74 (Table 1). The Al_2O_3 contents are lower than 1 wt% (Fig. 32 and Table 1). These differences in CaO and Al_2O_3 of low-Ca pyroxene may be due to the facts that the low-Ca pyroxene crystallized as orthopyroxene for barred-Ol-Px type and originally as protoenstatite for porphyritic to granular and radial-Px types. In Fig. 33, low-Ca pyroxenes in radial-Px chondrules are plotted, showing that there is a positive correlation between the FeO and Cr_2O_3 contents, which is also observed for enstatites in Qingzhen (EH3) (McKinley *et al.* 1984). This relation suggests that the precursors of radial-Px chondrules contained Cr as Cr_2O_3 in proportion to FeO and not as metallic Cr nor Cr-sulfides.

Secondary enstatites are nearly free from CaO, FeO, TiO_2, and Al_2O_3 (Appendices I and II). They are close to pure $MgSiO_3$ in chemical composition.

8.3. High-Ca pyroxene

High-Ca pyroxene is diopside and the Ca/(Ca+Mg+Fe) ratios range from 0.31 to 0.51 (Fig. 31). The Al_2O_3 contents are variable, ranging from 2 to 18 wt% (Fig. 32 and Table 1), and the Cr_2O_3 (0.2–3.4 wt%) and TiO_2 (0.2–1.9 wt%) contents of high-Ca pyroxene are slightly higher than those of coexisting primary low-Ca pyroxenes (Appendices I and II). For reference, compositional ranges of diopside and fassaite occurring in CAI's (types A and B) in Allende (Grossman, 1975) are shown in Fig. 32, and they are plotted along and slightly above the line between diopside and Ca-tschermak's molecule. In contrast, high-Ca pyroxenes in Y-691 chondrules are plotted below the line, being different in chemical composition from those in CAI's. Most high-Ca pyroxenes in Y-691 chondrules are primary pyroxenes which crystallized from residual melts, changing from Al-poor to Al-rich ones with decreasing temperature. But Al-poor diopsides in mesostasis of some chondrules seem to have fromed by decomposition of aluminous diopsides after chondrule solidification, and the secondary diopside is more magnesian than the primary Al-rich diopside, suggesting that the decomposition took place under a reducing condition.

8.4. Spinel

Spinel occurs in some barred-Ol-Px chondrules (Nos. 176, 264, 266 and 310). The TiO_2 content is nearly free. Spinels in chondrules Nos. 176, 264 and 266 are similar in chemical composition to each other with Cr/(Cr+Al) ratios of 0.02–0.006 and the *mg* values of 0.99–1.0. In contrast, spinel in chondrule No. 310 is different in Cr/(Cr+Al) (0.18) and the *mg* value (0.85) from those of the other chondrules. Spinels in barred-Ol-Px chondrules occur always in association with Al-rich phases such as aluminous diopside which crystallized from Al-rich residual melts of chondrules, suggesting that spinels were a latest-stage product of the crystalliza-

tion sequence of chondrules.

8.5. Plagioclase

Plagioclases in chondrules are genetically divided into two groups; primary and secondary. The former is plagioclases which crystallized directly from residual melts of chondrules, and the latter is albite which was produced after chondrule solidification from aluminous diopside (see Section 9.3). The primary plagioclase occurs in some chondrules and the compositions range from calcic to sodic. The secondary plagioclase is always close in chemical composition to Ca-free albite.

8.6. Silica minerals

Transparent-SiO_2 chondrules consist mainly of silica minerals. They often show low reflection index and low birefringence under a microscope, suggesting that they are crystobalite and/or tridymite. Some transparent-SiO_2 chondrules seem to be silica glass because they show no birefringence under a microscope.

Silica minerals occur in groundmasses of most radial-Px chondrules, and they are a latest-stage phase which crystallized from residual melts of chondrules enriched in SiO_2. In some cryptocrystalline chondrules, silica minerals occur as microphenocrysts and seems to have been a primary liquidus phase in the chondrules. Silica minerals in some cryptocrystalline chondrules seem to have grown from the rim towards the interior of chondrules (for examples, chondrules Nos. 138 and 151). They seem to have been a liquidus phase. Silica minerals observed at rim of some chondrules seem to have attached at the edge of chondrules from the outside. For examples, a silica mineral partly attaches at the edge of ferroan chondrule No. 154, and for the case of cryptocrystalline chondrule No. 215 a silica mineral completely surrounds the chondrule. The silica mineral surrounding chondrules may have grown on the chondrule edge from the ambient nebular gas after chondrule solidification and prior to the accretion.

8.7. Metals and sulfides

Metal and sulfide occur in small amounts probably less than a few volume percent in most Y-691 chondrules. Fe-metal and troilite in chondrules occur as primary and secondary phases. In some chondrules Fe-metal and troilite occur as small globules, which are considered to have formed by liquid immiscibility between silicate melts and metal-sulfide melts. Irregularly-shaped larger grains of Fe-metal, troilite, niningerite and/or oldhamite are observed in some chondrules, and they are primary. Chemical compositions of the Fe-metal and troilite (Appendix IV) are similar to those in opaque-mineral nodules (IKEDA, 1989). On the other hand, secondary Fe-metal and probably troilite in some chondrules occur after pseudomorph of ferroan olivine grains with Mg-silicates and are very small.

9. Discussion

9.1. Crystallization of chondrules

Barred-Ol-Px chondrules are mostly holocrystalline although porphyritic to

granular and radial-Px chondrules comprise clean or devitrified glasses in the groundmass. The generalized crystallization sequence of barred-Ol-Px chondrules is; (1) olivine, (2) low-Ca pyroxene, (3) high-Ca pyroxene, and (4) spinel or plagioclase, in the order of decreasing temperature. Olivine and pyroxene always occur in barred-Ol-Px chondrules although the other minerals are observed in some chondrules and lack in others. Spinel and Al-rich pyroxenes in barred-Ol-Px chondrules, Nos, 264, 176 and 266, crystallized from residual melts after rapid crystallization of olivine and Al-poor pyroxene, which changed the chemical composition of residual melts to be enriched in CaO, FeO, Al_2O_3, Cr_2O_3, TiO_2 and alkalies and to become poorer in SiO_2. In barred-Ol-Px chondrule No. 169, primary plagioclase occurs instead of Al-rich pyroxenes and spinel. SiO_2 content of the chondrule (SiO_2=52 wt%) is higher than that of the other barred-Ol-Px chondrules (IKEDA, 1988a), and the residual melt of the chondrule may have enriched in SiO_2 in comparison to the others.

Generalized crystallization sequence of porphyritic to granular chondrules is; (1) primary or relic olivine, (2) low-Ca pyroxene, (3) high-Ca pyroxene, and (4) plagioclase or glass. Low-Ca pyroxene is predominant in this type, and olivine is minor or lacking. High-Ca pyroxene occurs commonly in mesostasis in this type although the amounts are less than those in barred-Ol-Px chondrules. Primary plagioclase occurs in chondrules Nos. 117 and 149, and their chemical compositions are calcic to intermediate. On the other hand, clean or devitrified glass occurs instead of primary plagioclase in mesostasis of the other chondrules, and their chemical compositions correspond to intermediate to sodic plagioclase.

Generalized crystallization sequence of radial-Px chondrules is; (1) low-Ca pyroxene, (2) high-Ca pyroxene and silica minerals, and (3) sodic plagioclase or glass. Olivine occurs in some radial-Px chondrules as a relic mineral, showing corroded forms. High-Ca pyroxene occurs in mesostasis of some chondrules although the modal amount seems to be less than those in barred-Ol-Px and porphyritic to granular types. Silica minerals occur commonly in mesostasis of radial-Px chondrules and seem to have crystallized with diopside at the same time (Fig. 17b). Most radial-Px chondrules include primary plagioclase or glass, and the chemical compositions are close to intermediate to sodic plagioclase. A ferroan radial-Px chondrule No. 154 consists merely of low-Ca pyroxene, showing a normal zoning with *mg* values ranging from 0.91 to 0.74. This suggests that the precursor material of the chondrule consisted merely of ferroan pyroxene, and it melted probably by instantaneous superheating to form a melt droplet, which crystallized at a supercooling subsolidus condition to form the radial-Px texture with a normal zoning.

Cryptocrystalline chondrules show pale color to dark or opaque. The opacity depends upon the amount of small metal and sulfide grains which scattered throughout the cryptocrystalline chondrules. BSE images reveal the various submicroscopic textures. A cryptocrystalline chondrule, No. 219, shows a beautiful dendritic growth of pyroxene (Fig. 27b), indicating that it cooled rapidly after crystallization of phenocrystic silica minerals. Cryptocrystalline chondrules sometimes show concentric structures consisting of fine-grained pyroxene or silica-mineral mantle and cryptocrystalline core. The pyroxene mantle seems to have been formed by rapid growth of pyroxene needles from the edge of chondrules into the interior. A concentric

chondrule No. 138 consists of silica-mineral mantle and opaque massive core (Fig. 26). The silica-mineral mantle may also have formed by growth of the silica mineral as a liquidus phase from the edge of chondrule into the interior. The initial state of growth of silica minerals at the edge of chondrule can be observed in chondrule No. 151 (Fig. 24).

9.2. Ferroan-olivine decomposition

As already stated in the foregoing sections, ferroan olivine in chondrules decomposed into aggregates of Fe-metal and Mg-silicates. Olivines with the *mg* values larger than 0.95 remain fresh in the chondrules with some exceptions, and olivines with the *mg* values smaller than 0.95 show various degrees of decomposition.

There are three types of products by decomposition; (i) coarse-grained FeO-free enstatite and minor Fe-metal, (ii) fine-grained aggregates of Mg-silicates and Fe-metal showing striped patterns (namely, decomposed-olivine), and (iii) dusty olivine including many tiny Fe-metal grains. Type (ii) is commonly observed in unusual silicate-inclusions (IKEDA, 1988b) and in barred-Ol-Px chondrules. The initial stage of type (ii) decomposition is observed very well in chondrule No. 264 (Fig. 3b). Both types (i) and (ii) are observed in a barred-Ol-Px chondrule (for an example, chondrule No. 169). On the other hand, type (iii) is observed in the interior of large olivine grains in radial-Px chondrules (Nos. 100 and 307), and the *mg* values of olivine grains are about 0.96–0.97. This type is similar to dusty olivines in Qingzhen reported by RAMBALDI *et al.* (1983).

Decomposition of type (i) or (ii) is considered to have taken place in an extremely reducing gas after solidification of chondrules (IKEDA, 1988b), and the reaction is shown in the following two equations (IKEDA, 1988b);

$$\underset{\text{Ol}}{Fe_2SiO_4} + \underset{\text{Gas}}{2H_2} \longrightarrow \underset{\text{Met}}{2Fe} + \underset{\text{Gas}}{SiO_2} + \underset{\text{Gas}}{2H_2O} \qquad (1)$$

and

$$\underset{\text{Ol}}{Mg_2SiO_4} + \underset{\text{Gas}}{SiO_2} \longrightarrow \underset{\text{En}}{2MgSiO_3} \qquad (2)$$

The SiO_2 component in eq. (2) may be supplied from the same chondrule by eq. (1) and/or from the nebular gas surrounding the chondrule. When SiO_2 component can be supplied both from eq. (1) and from the ambient gas, the reaction (2) may form abundant amounts of enstatite with minor Fe-metal. The coarse-grained FeO-free enstatite of the occurrence (i) was, thus, formed. If SiO_2 component of the ambient gas was not supplied, the SiO_2 component in eq. (2) would be supplied from the right hand side of eq. (1). In this case, the bulk composition of "decomposed-olivine grains" should be equal to that of original ferroan olivine grains except for oxygen content. This is the case for fine-grained aggregates of Mg-silicates and Fe-metal showing striped patterns in unusual silicate-inclusions (IKEDA, 1988b). The decomposed-olivine of the occurrence (ii) in barred-Ol-Px chondrules may also have formed in the same manner. Ferroan olivine with the *mg* values of 0.92–0.93 in chondrule No. 310 has not suffered from the reaction, suggesting that the chondrule

had been exposed in a reducing nebular gas only for short period which may have prevented the reaction of eqs. (1) and (2).

On the other hand, type (iii) decomposition is limited in central portion of large olivine grains in radial-Px chondrules, and the rim of the olivine grains remains fresh. This suggests that the dusty olivine cores were originally relic olivine with more ferroan compositions than the rim. During melting events and subsequent crystallization, the ferroan olivine decomposed at high temperatures into tiny Fe-metal grains and more magnesian olivine corresponding to the rim olivine. The possible reaction equation (RAMBALDI *et al.*, 1983) is;

$$\underset{\text{Ol}}{Fe_2SiO_4} + 2\,\underset{\text{Melt}}{MgO} \longrightarrow \underset{\text{Ol}}{Mg_2SiO_4} + 2\,\underset{\text{Met}}{Fe} + \underset{\text{Gas}}{O_2} \qquad (3)$$

If so, the fundamental difference between type (iii) and the other two is that the reaction for type (iii) took place during melting whereas the reactions for types (i) and (ii) did at subsolidus temperatures.

9.3. Albite formation

There are two types of albite occurrence in Y-691 chondrules; (1) in mesostasis, and (2) in peripheral portions of chondrules. The former type is primary albite which crystallized from the residual melts of chondrules. On the other hand, the latter type is close to pure albite in chemical composition, and appears to have replaced aluminous diopsides after chondrule solidification by introduction of alkalies and silica from the ambient nebular gas. The reaction is shown in the following equation:

$$\underset{\text{CaT}}{CaAl_2SiO_6} + 1/2\,\underset{\text{Fo}}{Mg_2SiO_4} + \underset{\text{Gas}}{Na_2O} + 6.5\,\underset{\text{Gas}}{SiO_2} \longrightarrow 2\,\underset{\text{Ab}}{NaSi_3AlO_8} + \underset{\text{Di}}{CaMgSi_2O_6} \qquad (4)$$

where CaT, Fo, Ab, and Di are calcium tschermak's molecule in aluminous diopside, forsterite molecule in olivine, secondary albite, and secondary diopside, respectively. The reaction is considered to have taken place in an extremely reducing gas because similar pure albite occurs commonly in opaque-mineral nodules which were produced in an extremely reducing gas (IKEDA, 1989).

9.4. Magnesian and ferroan spinel formation

Spinel occurs in some barred-Ol-Px chondrules. The *mg* values of the spinel range from 1.0–0.99 in chondrules Nos. 264, 176 and 266 to 0.84 in chondrule No. 310. The occurrence of spinels suggests that they originally crystallized from residual melts with Al-rich pyroxenes. However, the *mg* values of coexisting Al-rich pyroxenes are smaller than those of spinels except for the case of chondrule No. 310. Therefore, the magnesian spinels with the *mg* values of 0.99–1.00 may have been originally more ferroan, the chondrules were brought into an extremely reduced gas after solidification, and the diffusional exchange of Mg and Fe between the spinel and the ambient gas caused formation of the magnesian spinels without remarkable change in pyroxene. In the case of chondrule No. 310, the diffusional exchange was not enough to produce magnesian spinel. Considering the fact that ferroan olivine (mg=0.92–0.93) in No. 310 remains fresh, the chondrule may have not experienced a long-period exposure

to the ambient reducing gas in comparison to the other chondrules.

9.5. Precursors of chondrules

Bulk compositions of chondrules reflect their precursors. Neglecting minor modification in chemical composition of chondrules which may have taken palce after solidification, precursors of barred-Ol-Px type contained the most abundant refractory components (CaO, Al_2O_3, etc.) and FeO in comparison to that of porphyritic to granular and radial-Px types with a few exceptions (IKEDA, 1988a). This difference results in modal amounts of aluminous pyroxene and spinel in chondrules and in compositional difference in CaO and FeO contents of olivines as shown in Fig. 30. On the other hand, SiO_2 and alkalies in the precursors were the most abundant in radial-Px type, moderate in porphyritic to granular type, and the least in barred-Ol-Px type (IKEDA, 1988a). This difference results in the facts that silica minerals occur abundantly in groundmass of radial-Px chondrules in contrast with the common occurrence of spinel in barred-Ol-Px chondrules and that plagioclase or glass in groundmass is sodic for most radial-Px chondrules in contrast with calcic to intermediate plagioclase in barred-Ol-Px chondrules. These systematic differences in chemical compositions of chondrules suggest that the precursors of barred-Ol-Px type were higher-temperature condensates and those of porphyritic to granular and radial-Px types were lower-temperature condensates.

Spherulitic subtype of cryptocrystalline chondrules shows a wide chemical compositions (IKEDA, 1988a), which overlap every type of chondrules. Most of spherulitic subtype are smaller than about 200 μm across, always showing spherical outlines. The spherulitic subtype may have formed in rapid cooling conditions from melt droplets which were stripped off by friction with nebular gas from larger chondrule melt drops splashing during collision of two planetesimals in protosolar nebula (KIEFFER, 1975).

Transparent-SiO_2 chondrules are observed only in enstatite chondrites. Their precursors might be silica minerals condensed directly from a gas which was enriched in Si by fractional condensation of high-temperature components such as forsterite and/or niningerite. Another possibility is that they were produced by the following reaction;

$$\underset{\text{Met}}{\text{Si}}+\underset{\text{Gas}}{2\text{H}_2\text{O}} \longrightarrow \underset{\text{Sil}}{\text{SiO}_2}+\underset{\text{Gas}}{2\text{H}_2} \qquad (5)$$

where Met is silicon in Fe-metal. Fe-metal in opaque-mineral nodules in Y-691 contains about 2 wt% Si, and they often occur in association with silica minerals (IKEDA, 1989). The Fe-metals might have originally contained more Si prior to the reaction (5). Chondrules No. 154 and 215 are partly or completely surrounded by silica minerals which seem to have grown from outside of the chondrules. This suggests that at least some fraction of silica minerals precipitated after solidification of chondrules and that the formation of transparent-SiO_2 chondrules might be the latest event of chondrule formation.

10. Summary

The Y-691 enstatite chondrite includes various textural types of chondrules. Radial-Px type is the largest and most abundant. Barred-Ol-Px, porphyritic to granular and cryptocrystalline types are common. Transparent-SiO_2 type occurs in small amounts.

Barred-Ol-Px type includes the most abundant olivine, porphyritic to granular type moderate, and radial-Px type the least. In contrast, the radial-Px type contains the most abundant silica minerals, which are free in barred-Ol-Px chondrules. Amounts of Ca- and/or Al-bearing phases such as Al-rich pyroxene and spinel are the most abundant in barred-Ol-Px type, and are the least in radial-Px type.

Crystallization for barred-Ol-Px chondrules began with olivine and low-Ca pyroxene, and the residual melts were enriched in CaO and Al_2O_3 to crystallize aluminous pyroxene, spinel and/or plagioclase. Prophyritic to granular chondrules crystallized olivine, low-Ca pyroxene, high-Ca pyroxene, and plagioclase (or glass) in this order. In radial-Px chondrules crystallization of low-Ca pyroxene changed the residual melts to SiO_2-rich ones, resulting in abundant amounts of silica minerals in the groundmass. In some cryptocrystalline chondrules silica minerals are a first liquidus phase.

Chondrule precursors of barred-Ol-Px type were produced from higher-temperature condensates in comparison to those of porphyritic to granular and radial-Px types. After or during formation of precursors, melting events took place to produce barred-Ol-Px chondrules. After solidification, they were brought into reducing nebular gases, where magnesian chondrules of porphyritic to granular and radial-Px types had been produced. Ferroan olivines in barred-Ol-Px chondrules decomposed into aggregates of Mg-silicates and Fe-metal, and ferroan spinel changed to magnesian one although some ferroan chondrules did not suffer from these reactions probably because of short-period exposure to the ambient reducing gas. Secondary albite was also produced in the peripheral portions of the barred-Ol-Px chondrules from aluminous diopside by introduction of alkalies and silica from the ambient reducing gas.

Silica minerals were a precursor material of radial-Px and transparent-SiO_2 chondrules, and they might have been produced by fractional condensation and/or oxidation of metallic silicon in Fe-metals.

Acknowledgments

I would like to express my thanks to NIPR for the Y-691 sample preparation and co-operation with the consortium on Y-691. This study has been supported by a Grant in Aid for Scientific Research, from the Ministry of Education, Science and Culture.

References

BENCE, A. E. and ALBEE, A. L. (1967): Empirical correction factors for the electron microanalysis of silicates and oxides. J. Geol., **76**, 382–403.

GROSSMAN, L. (1975): Petrology and mineral chemistry of Ca-rich inclusions in the Allende meteorite. Geochim. Cosmochim. Acta, **39**, 433–451.

IKEDA, Y. (1988a): Petrochemical study of the Y-691 enstatite chondrite (E3) I; Major element chemical compositions of chondrules and inclusions. Proc. NIPR Symp. Antarct. Meteorites, **1**, 3–13.

IKEDA, Y. (1988b): Petrochemical study of the Y-691 enstatite chondrite (E3) II; Descriptions and mineral compositions of unusual silicate-inclusions. Proc. NIPR Symp. Antarct. Meteorites, **1**, 14–37.

IKEDA, Y. (1989): Petrochemical study of the Y-691 enstatite chondrite (E3) IV; Descriptions and mineral chemistry of opaque-mineral nodules. Proc. NIPR Symp. Antarct. Meteorites, **2**, 109–146.

KEIFFER, S. W. (1975): Droplet chondrules. Science, **189**, 333–340.

MCKINLEY, S. G., SCOTT, E. R. D. and KEIL, K. (1984): Composition and origin of enstatite in E chondrites. Proc. Lunar Planet. Sci. Conf., 14th, Part 2, B567–B572 (J. Geophys. Res., Suppl.).

OKADA, A. (1975): Petrological studies of the Yamato meteorites. Part I; Mineralogy of the Yamato meteorites. Mem. Natl Inst. Polar Res., Spec. Issue, **5**, 14–66.

OKADA, A., YAGI, Y. and SHIMA, M. (1975): Petrological studies of the Yamato meteorites. Part II; Petorology of the Yamato meteorites. Mem. Natl Inst. Polar Res., Spec. Issue, **5**, 67–82.

RAMBALDI, E. R., RAJAN, R. S., WANG, D. and HOUSLEY, R. M. (1983): Evidence of relict grains in chondrules of Qingzhen, and E3 type enstatite chondrites. Earth Planet. Sci. Lett., **66**, 11–24.

(Received April 15, 1988; Revised manuscript received October 11, 1988)

Appendix I

Chemical compositions of the constituents in barred-Ol-Px chondrules and the affinity. Ol, dOl, En, sEn, Br, Fas, Di, Sp, and Pl are olivine, decomposed-olivine, primary enstatite, secondary enstatite, bronzite, fassaitic diopside ($Al_2O_3 > 10$ wt%), diopside ($Al_2O_3 < 10$ wt%), spinel, and plagioclase, respectively.

	1	2	3	4	5	6	7	8	9	10	11	12
1		120	120	120	120	120	120	120	120	120	169	169
2		Di	Di	Di	En	En	En	En	Ol	Ol	Br	Br
3	SiO2	49.86	49.98	51.79	54.57	55.43	55.04	55.09	39.74	40.04	52.09	53.94
4	TiO2	0.56	0.50	0.35	0.29	0.22	0.25	0.13	0.00	0.04	0.26	0.15
5	Al2O3	8.14	5.55	4.62	4.92	4.00	3.95	2.16	0.00	0.00	4.73	3.08
6	Cr2O3	0.92	0.75	0.56	0.73	0.57	0.75	0.59	0.16	0.26	1.42	1.24
7	FeO	1.33	1.47	1.62	1.99	1.92	1.98	2.47	3.29	3.62	10.56	10.31
8	MnO	0.20	0.13	0.08	0.10	0.00	0.16	0.00	0.00	0.11	0.57	0.44
9	MgO	18.35	20.79	20.85	35.45	34.82	34.62	35.43	55.31	54.83	28.30	30.08
10	CaO	20.51	19.42	19.95	2.21	2.69	3.01	2.39	0.28	0.18	2.08	1.91
11	Na2O	0.00	0.00	0.04	0.00	0.00	0.00	0.00	0.00	0.00	0.00	0.08
12	K2O	0.00	0.00	0.03	0.00	0.00	0.00	0.00	0.00	0.00	0.00	0.00
13	Total	99.87	98.59	99.89	100.26	99.65	99.76	98.26	98.78	99.08	100.01	101.23

	13	14	15	16	17	18	19	20	21	22	23	24
1	169	169	169	169	169	169	169	169	169	169	169	169
2	Br	Br	Br	Br	Br	Br	Br	Br	Br	Br	Br	Br
3	54.90	53.39	55.72	53.62	52.86	55.01	55.36	55.97	55.79	54.96	54.78	55.86
4	0.14	0.25	0.14	0.22	0.16	0.15	0.12	0.08	0.09	0.08	0.11	0.07
5	1.33	1.67	1.66	1.56	1.49	1.23	1.16	1.11	1.07	0.94	0.90	0.84
6	0.81	0.71	0.93	0.90	0.84	0.63	0.72	0.72	0.80	0.81	0.65	0.73
7	10.23	12.06	8.19	9.66	10.75	8.13	9.11	9.19	9.09	9.18	10.42	9.54
8	0.26	0.28	0.36	0.15	0.00	0.21	0.12	0.15	0.17	0.32	0.23	0.35
9	31.75	29.41	32.70	31.57	31.13	32.80	32.91	33.02	33.18	32.36	31.63	31.70
10	1.55	2.17	1.18	1.20	1.52	1.15	0.87	1.01	0.93	0.93	1.25	1.03
11	0.11	0.12	0.00	0.17	0.11	0.05	0.00	0.00	0.00	0.09	0.00	0.03
12	0.02	0.00	0.00	0.05	0.00	0.00	0.00	0.00	0.00	0.00	0.00	0.00
13	101.10	100.06	100.88	99.10	98.86	99.36	100.37	101.25	101.12	99.67	99.97	100.15

	25	26	27	28	29	30	31	32	33	34	35	36
1	169	169	169	169	169	169	169	169	169	176	176	176
2	sEn	sEn	sEn	sEn	sEn	Pl	Pl	Pl	dOl	Sp	Fas	Di
3	58.26	58.31	57.61	57.34	58.79	47.35	47.24	46.09	38.10		47.46	50.08
4	0.06	0.06	0.00	0.00	0.00	0.12	0.03	0.05	0.00	0.00	0.55	0.34
5	0.07	0.09	0.19	0.06	0.07	32.02	30.93	32.11	0.00	68.60	13.03	8.29
6	0.03	0.00	0.00	0.09	0.01	0.00	0.08	0.00	0.22	1.92	0.37	0.32
7	0.31	0.25	0.26	0.28	0.44	0.51	0.99	0.69	7.84	0.35	1.12	1.24
8	0.08	0.00	0.00	0.00	0.05	0.00	0.00	0.00	0.25	0.00	0.00	0.00
9	41.14	41.29	41.80	40.99	41.26	2.20	2.86	1.73	55.91	28.14	15.46	19.26
10	0.11	0.10	0.06	0.00	0.11	14.49	14.33	14.00	0.07	0.09	22.32	20.19
11	0.06	0.12	0.09	0.00	0.00	3.05	2.95	3.67	0.11		0.00	0.26
12	0.02	0.07	0.00	0.00	0.00	0.13	0.07	0.11	0.00		0.00	0.04
13	100.14	100.29	100.01	98.76	100.73	99.87	99.48	98.45	102.50	99.10	100.31	100.02

	37	38	39	40	41	42	43	44	45	46	47	48
1	176	176	176	176	176	176	176	176	176	176	176	176
2	Di	Di	Di	Di	Di	En	En	En	En	En	En	En
3	49.64	51.51	51.83	53.31	53.96	52.88	54.61	55.38	55.90	56.08	57.35	56.61
4	0.66	0.50	0.36	0.42	0.27	0.39	0.21	0.20	0.19	0.21	0.16	0.25
5	6.86	5.60	5.47	2.98	2.15	9.31	3.95	3.87	2.74	2.63	2.41	2.11
6	0.98	0.73	0.21	0.60	0.47	0.61	0.81	0.71	0.55	0.62	0.62	0.64
7	1.28	1.24	1.34	1.20	1.17	2.06	1.85	2.13	1.77	1.76	1.76	1.92
8	0.10	0.00	0.00	0.00	0.00	0.00	0.07	0.20	0.15	0.10	0.00	0.00
9	18.58	19.53	19.66	20.34	22.48	33.89	35.72	35.08	35.35	35.13	36.12	35.68
10	20.69	20.72	19.89	20.58	18.82	2.03	2.17	2.14	2.32	2.64	2.49	2.79
11	0.08	0.00	0.00	0.00	0.00	0.00	0.00	0.00	0.00	0.00	0.00	0.00
12	0.04	0.00	0.00	0.05	0.00	0.00	0.00	0.00	0.00	0.00	0.00	0.00
13	98.91	99.83	98.76	99.48	99.32	101.17	99.39	99.71	98.97	99.17	100.91	100.00

	49	50	51	52	53	54	55	56	57	58	59	60
1	176	176	176	176	176	259	259	259	259	259	259	259
2	En	Ol	Ol	Ol	Ol	Fas	Di	Di	En	En	En	Ol
3	56.06	41.18	41.57	41.71	41.60	48.86	49.26	48.48	52.74	52.73	54.56	40.67
4	0.26	0.00	0.00	0.00	0.00	0.57	0.55	0.67	0.24	0.37	0.28	0.03
5	1.82	0.00	0.00	0.00	0.00	10.13	7.97	9.87	7.92	5.61	4.03	0.10
6	0.62	0.04	0.06	0.04	0.06	0.87	0.74	0.84	1.00	0.77	0.66	0.13
7	1.58	3.67	3.20	3.74	3.79	2.63	2.36	2.61	3.35	3.50	4.46	4.82
8	0.23	0.13	0.07	0.08	0.00	0.14	0.09	0.00	0.00	0.22	0.10	0.06
9	35.80	54.36	54.21	54.51	54.64	17.87	19.82	17.69	32.56	34.79	33.50	52.73
10	2.50	0.24	0.19	0.23	0.21	19.48	18.13	18.92	2.15	2.83	2.52	0.21
11	0.00	0.00	0.00	0.00	0.00	0.00	0.00	0.00	0.00	0.06	0.00	0.00
12	0.03	0.00	0.00	0.00	0.00	0.00	0.00	0.00	0.00	0.00	0.00	0.00
13	98.90	99.62	99.30	100.31	100.30	100.55	98.92	99.08	99.96	100.88	100.11	98.75

	61	62	63	64	65	66	67	68	69	70	71	72
1	259	259	264	264	264	264	264	264	264	264	264	264
2	Ol	Ol	Sp	Sp	Fas	Fas	Fas	Fas	Fas	Fas	Fas	Fas
3	40.59	40.16			44.48	45.71	45.13	45.79	45.34	45.58	46.71	46.80
4	0.00	0.00	0.08	0.03	0.23	0.84	0.87	0.66	1.26	0.62	0.58	1.03
5	0.05	0.00	71.82	69.15	17.89	15.98	15.86	15.04	14.93	14.48	14.17	13.44
6	0.10	0.21	0.70	1.84	0.25	0.26	0.38	0.31	0.95	0.28	0.22	0.67
7	4.45	4.65	0.11	0.55	1.77	1.39	1.45	1.46	1.84	1.49	1.74	2.04
8	0.00	0.00	0.00	0.17	0.00	0.00	0.00	0.14	0.00	0.00	0.00	0.00
9	54.19	54.32	28.00	29.53	14.53	15.65	14.78	15.84	15.54	15.68	16.95	16.07
10	0.16	0.28	0.00	0.18	20.65	21.34	21.45	20.63	20.70	20.89	20.47	20.67
11	0.00	0.00			0.00	0.06	0.04	0.00	0.00	0.00	0.00	0.06
12	0.10	0.00			0.00	0.00	0.03	0.02	0.00	0.04	0.00	0.00
13	99.64	99.62	100.71	101.45	99.80	101.23	99.99	99.89	100.56	99.06	100.84	100.78

	73	74	75	76	77	78	79	80	81	82	83	84
1	264	264	264	264	264	264	264	264	264	264	264	264
2	Fas	Di	Di	Di	En	En	En	En	En	En	En	En
3	46.44	50.72	51.86	51.19	49.51	49.86	51.56	50.22	50.68	55.10	54.33	54.92
4	0.58	0.62	0.58	0.49	0.34	0.47	0.55	0.47	0.32	0.31	0.19	0.28
5	13.98	7.36	5.29	4.33	13.58	12.03	11.62	11.46	10.94	4.56	4.01	3.91
6	0.24	0.77	1.07	1.00	0.04	0.85	1.00	0.92	0.20	0.94	1.14	1.00
7	2.28	1.40	2.09	2.68	3.01	2.87	2.91	2.97	3.02	2.38	2.40	2.80
8	0.13	0.00	0.08	0.00	0.00	0.06	0.00	0.00	0.11	0.13	0.00	0.10
9	16.14	19.96	22.80	21.86	31.41	32.16	31.43	32.20	32.04	35.15	34.56	34.17
10	20.68	19.30	16.09	16.85	2.88	1.98	2.33	2.06	2.84	2.44	2.49	2.74
11	0.00	0.00	0.00	0.07	0.00	0.00	0.03	0.00	0.00	0.04	0.05	0.00
12	0.00	0.00	0.00	0.00	0.00	0.02	0.00	0.00	0.06	0.00	0.00	0.00
13	100.47	100.13	99.86	98.47	100.77	100.30	101.43	100.30	100.21	101.05	99.17	99.92

	85	86	87	88	89	90	91	92	93	94	95	96
1	264	264	264	264	264	264	264	264	264	264	266	266
2	En	En	En	En	En	En	Ol	Ol	Ol	Ol	Sp	Fas
3	55.12	55.34	55.37	55.56	55.75	55.71	40.41	40.08	39.27	42.10		47.23
4	0.30	0.26	0.19	0.23	0.24	0.20	0.00	0.00	0.00	0.00	0.02	0.58
5	3.82	3.58	3.15	2.97	2.54	2.44	0.00	0.06	0.00	0.00	68.10	14.09
6	0.81	0.98	0.93	0.92	0.94	0.93	0.21	0.23	0.22	0.10	2.12	0.56
7	2.92	2.63	2.72	2.61	3.04	2.77	4.74	5.62	5.73	4.22	0.53	1.31
8	0.28	0.07	0.00	0.00	0.00	0.00	0.08	0.00	0.00	0.24	0.00	0.00
9	34.82	35.63	35.53	33.54	35.47	36.00	54.86	54.09	54.59	51.38	27.17	16.64
10	2.86	2.55	2.40	2.28	2.46	2.20	0.30	0.26	0.37	0.45	0.07	19.59
11	0.04	0.00	0.00	0.00	0.00	0.00	0.04	0.00	0.00	0.00		0.13
12	0.00	0.00	0.00	0.00	0.00	0.00	0.03	0.00	0.00	0.00		0.00
13	100.97	101.04	100.29	98.11	100.44	100.25	100.67	100.34	100.18	98.49	98.01	100.13

	97	98	99	100	101	102	103	104	105	106	107	108
1	266	266	266	266	266	266	266	266	266	266	266	266
2	Fas	Fas	Di	Di	Di	Di	Di	Di	Di	Di	En	En
3	47.49	47.41	51.35	51.27	50.97	49.76	50.56	50.24	52.08	52.26	53.99	53.11
4	0.31	0.45	0.54	0.55	0.52	0.50	0.47	0.79	0.44	0.40	0.24	0.19
5	13.95	13.58	7.90	7.54	7.44	7.39	6.69	6.55	5.69	4.79	6.80	6.22
6	0.59	0.63	1.04	0.97	1.20	0.79	0.82	1.26	0.83	0.81	0.72	1.25
7	1.45	1.56	1.43	1.54	1.72	1.61	1.65	1.89	1.81	1.88	2.65	2.38
8	0.00	0.00	0.07	0.00	0.00	0.09	0.12	0.09	0.00	0.00	0.18	0.07
9	17.03	16.70	18.75	19.58	20.52	19.43	21.14	19.21	21.76	21.24	33.06	33.88
10	19.83	19.24	19.50	19.17	17.78	18.94	16.67	20.14	16.60	17.30	2.48	2.04
11	0.00	0.06	0.00	0.00	0.16	0.00	0.16	0.00	0.00	0.00	0.00	0.00
12	0.00	0.00	0.00	0.00	0.00	0.05	0.06	0.00	0.00	0.00	0.00	0.02
13	100.65	99.63	100.58	100.62	100.31	98.56	98.34	100.17	99.21	98.68	100.12	99.16

	109	110	111	112	113	114	115	116	117	118	119	120
1	266	266	266	266	266	266	266	266	266	266	266	266
2	En	En	En	En	En	En	En	En	Ol	Ol	Ol	Ol
3	54.13	55.26	55.11	52.20	54.51	54.80	54.70	56.36	41.24	41.07	41.53	41.54
4	0.35	0.25	0.29	0.32	0.29	0.22	0.25	0.26	0.00	0.00	0.00	0.00
5	5.97	4.56	4.13	4.10	4.10	3.56	3.12	2.17	0.02	0.00	0.00	0.00
6	0.85	1.15	0.94	1.19	1.10	0.96	1.01	0.84	0.12	0.09	0.04	0.08
7	2.51	2.75	2.80	2.80	2.56	2.99	2.96	3.14	4.24	3.99	3.23	3.03
8	0.10	0.00	0.00	0.13	0.00	0.00	0.08	0.00	0.06	0.00	0.00	0.00
9	34.39	34.04	34.20	37.14	34.62	34.16	35.48	34.60	54.57	54.41	54.46	55.11
10	2.01	2.59	2.51	1.93	2.45	2.36	2.08	2.72	0.21	0.16	0.24	0.21
11	0.00	0.00	0.00	0.00	0.00	0.00	0.00	0.00	0.09	0.00	0.05	0.00
12	0.00	0.00	0.00	0.00	0.00	0.00	0.04	0.00	0.00	0.00	0.00	0.00
13	100.31	100.60	99.98	99.81	99.63	99.05	99.72	100.09	100.55	99.72	99.55	99.97

	121	122	123	124	125	126	127	128	129	130	131	132
1	266	266	267	267	267	267	267	267	267	310	310	310
2	Ol	Ol	Di	Di	En	En	En	Ol	Ol	Sp	Fas	Fas
3	41.23	41.20	48.99	50.21	53.91	52.89	52.25	41.59	41.80		45.11	45.91
4	0.00	0.00	0.70	0.84	0.41	0.34	0.37	0.04	0.04	0.22	1.47	1.37
5	0.00	0.00	9.51	7.97	7.34	9.06	8.57	0.00	0.00	53.04	13.56	12.35
6	0.08	0.06	0.42	0.50	0.52	0.61	0.52	0.14	0.21	17.29	1.41	1.15
7	4.11	4.08	1.13	0.81	1.03	0.85	1.21	1.54	1.68	7.16	2.00	2.46
8	0.00	0.12	0.00	0.09	0.00	0.00	0.00	0.00	0.00	0.00	0.00	0.00
9	53.11	54.02	20.04	19.65	34.47	34.17	34.96	56.85	55.98	22.41	13.45	14.18
10	0.21	0.20	19.39	20.16	2.29	1.66	1.86	0.19	0.22	0.43	22.64	23.60
11	0.00	0.00	0.00	0.00	0.00	0.00	0.00	0.00	0.00		0.00	0.00
12	0.06	0.00	0.00	0.00	0.00	0.00	0.00	0.00	0.00		0.00	0.00
13	98.80	99.68	100.18	100.23	99.97	99.58	99.74	100.35	99.93	100.55	99.64	101.02

	133	134	135	136	137	138
1	310	310	310	310	310	310
2	Di	Di	Ol	Ol	Ol	Ol
3	47.39	51.51	40.69	40.54	40.36	40.25
4	0.91	0.63	0.05	0.14	0.04	0.08
5	9.96	5.31	0.18	0.45	0.30	0.06
6	0.72	0.41	0.04	0.08	0.21	0.15
7	2.86	2.54	7.36	6.82	7.16	6.89
8	0.22	0.11	0.29	0.00	0.00	0.19
9	15.32	18.05	50.36	50.52	52.33	52.08
10	21.95	22.07	0.28	0.32	0.36	0.50
11	0.00	0.00	0.04	0.00	0.03	0.00
12	0.00	0.00	0.00	0.00	0.00	0.00
13	99.33	100.63	99.29	98.87	100.79	100.20

Appendix II

Chemical compositions of the constituents in porphyritic or granular chondrules (Nos. 109, 110, 115, 117, 149, 158, 159, 238, and 244) and radial-Px chondrules (Nos. 100, 101, 102, 116, 124, 126, 127, 128, 137, 154, 161, 175, 268, and 307). Ol, dOl, En, sEn, Br, Fas, Di, Pl, Ab, Silica, rimQz, Gl, and dGl are olivine, decomposed-olivine, primary enstatite, secondary enstatite, bronzite, fassaitic diopside, diopside, plagioclase, albite, silica mineral, silica mineral at chondrule rims, glass, and devitrified glass, respectively.

	1	2	3	4	5	6	7	8	9	10	11	12
1		109	109	109	109	109	109	109	109	109	109	109
2		Ol	Ol	En	En	En	En	En	En	Gl	Gl	Gl
3	SiO2	41.83	42.11	59.66	58.43	58.84	58.46	57.97	58.57	62.22	67.63	66.74
4	TiO2	0.07	0.00	0.08	0.12	0.09	0.20	0.09	0.00	0.53	0.28	0.28
5	Al2O3	0.00	0.00	0.06	0.22	0.23	0.66	0.45	0.23	16.74	14.30	14.53
6	Cr2O3	0.33	0.31	0.27	0.34	0.31	0.46	0.42	0.30	0.08	0.00	0.00
7	FeO	0.75	0.67	1.06	0.78	0.52	0.39	0.58	0.68	0.10	0.12	0.00
8	MnO	0.00	0.12	0.00	0.12	0.00	0.13	0.17	0.00	0.00	0.00	0.00
9	MgO	57.08	57.46	39.58	40.10	39.86	39.50	40.07	40.42	7.19	7.02	6.54
10	CaO	0.13	0.05	0.12	0.14	0.15	0.39	0.30	0.23	0.45	0.28	0.21
11	Na2O	0.00	0.00	0.00	0.00	0.00	0.00	0.00	0.00	9.96	8.05	8.68
12	K2O	0.00	0.00	0.00	0.00	0.00	0.00	0.00	0.00	2.02	1.80	2.24
13	Total	100.19	100.72	100.83	100.25	100.00	100.19	100.05	100.43	99.29	99.48	99.22

	13	14	15	16	17	18	19	20	21	22	23	24
1	110	110	110	110	110	110	110	110	110	115	115	115
2	Ol	Ol	Ol	Ol	En	En	En	En	En	Ol	En	En
3	41.05	41.23	41.30	41.34	58.69	60.22	58.91	59.13	58.75	41.86	59.55	59.16
4	0.03	0.05	0.00	0.00	0.05	0.05	0.05	0.08	0.09	0.00	0.14	0.00
5	0.00	0.00	0.00	0.00	0.33	0.21	0.22	0.03	0.02	0.00	0.17	0.28
6	0.35	0.34	0.32	0.29	0.58	0.31	0.50	0.38	0.43	0.37	0.32	0.31
7	1.22	1.30	0.96	1.27	0.77	0.86	0.77	1.13	0.95	1.09	0.53	0.88
8	0.12	0.14	0.22	0.24	0.33	0.00	0.23	0.10	0.25	0.00	0.16	0.23
9	56.52	56.44	57.72	57.22	39.87	38.08	37.95	38.96	38.35	58.28	39.97	39.18
10	0.06	0.09	0.04	0.02	0.23	0.31	0.21	0.25	0.37	0.10	0.36	0.19
11	0.00	0.05	0.03	0.00	0.00	0.04	0.00	0.00	0.00	0.00	0.03	0.00
12	0.00	0.00	0.00	0.00	0.00	0.04	0.00	0.00	0.00	0.00	0.03	0.00
13	99.35	99.64	100.59	100.38	100.85	100.12	98.84	100.06	99.21	101.70	101.26	100.23

	25	26	27	28	29	30	31	32	33	34	35	36
1	115	115	115	115	115	115	117	117	117	117	117	117
2	En	En	En	En	Gl	Gl	Ol	Ol	Ol	En	En	En
3	58.13	58.16	58.70	57.97	60.02	58.57	43.05	41.20	41.42	58.38	59.09	58.88
4	0.09	0.00	0.03	0.09	0.37	0.31	0.07	0.00	0.02	0.31	0.03	0.05
5	0.31	0.24	0.33	0.29	18.39	20.93	0.29	0.02	0.02	0.36	0.06	0.40
6	0.34	0.36	0.37	0.40	0.21	0.09	0.26	0.33	0.37	0.42	0.36	0.56
7	0.84	0.84	0.73	1.09	0.48	0.26	0.71	0.90	0.89	1.31	1.01	1.50
8	0.09	0.11	0.23	0.15	0.04	0.40	0.00	0.04	0.00	0.13	0.00	0.16
9	40.04	40.10	39.69	39.05	5.48	5.65	55.40	57.92	57.53	38.40	38.48	39.88
10	0.21	0.16	0.20	0.12	7.08	9.49	0.23	0.13	0.17	0.21	0.27	0.42
11	0.03	0.02	0.04	0.00	6.00	4.07	0.10	0.00	0.00	0.08	0.00	0.06
12	0.00	0.00	0.00	0.00	0.50	0.22	0.00	0.00	0.00	0.00	0.00	0.00
13	100.08	99.99	100.32	99.16	98.57	99.99	100.11	100.54	100.42	99.60	99.30	101.91

	37	38	39	40	41	42	43	44	45	46	47	48
1	117	117	117	117	149	149	149	149	149	149	149	149
2	Fas	Fas	Pl	Pl	Ol	Ol	Ol	En	En	En	Di	Di
3	47.18	47.71	48.75	50.62	40.93	41.08	41.23	57.55	58.01	58.00	50.19	53.51
4	1.66	1.59	0.00	0.00	0.00	0.00	0.00	0.00	0.00	0.00	0.84	0.73
5	10.34	12.70	32.86	31.06	4.00	0.03	0.00	0.43	0.26	0.45	9.23	2.83
6	0.38	0.45	0.00	0.00	0.31	0.29	0.25	0.26	0.31	0.37	0.64	0.52
7	0.30	0.35	0.19	0.24	1.03	0.89	0.89	0.64	0.62	0.82	1.24	0.56
8	0.14	0.00	0.22	0.00	0.23	0.45	0.36	0.28	0.39	0.16	0.80	0.70
9	16.91	17.28	0.81	0.07	56.61	57.18	57.50	39.85	39.87	39.22	15.42	22.15
10	21.02	21.22	15.03	16.34	0.13	0.20	0.13	0.23	0.33	0.27	20.36	18.64
11	0.16	0.07	2.13	1.73	0.08	0.04	0.05	0.00	0.00	0.00	0.51	0.06
12	0.05	0.07	0.08	0.00	0.00	0.00	0.09	0.05	0.00	0.00	0.10	0.06
13	98.14	101.44	100.07	100.06	103.32	100.16	100.50	99.29	99.79	99.29	99.33	99.76

	49	50	51	52	53	54	55	56	57	58	59	60
1	149	158	158	158	158	159	159	159	159	238	238	238
2	Pl	En	En	En	Gl	Ol	Ol	Ol	En	En	En	Di
3	60.27	57.93	57.96	57.82	67.22	40.88	41.46	41.48	59.20	59.61	59.05	53.15
4	0.16	0.00	0.00	0.04	0.11	0.00	0.00	0.00	0.08	0.00	0.00	1.49
5	23.34	0.91	0.45	0.67	19.88	0.00	0.00	0.09	0.95	0.20	0.71	4.04
6	0.09	0.08	0.36	0.18	0.00	0.35	0.34	0.17	0.52	0.49	0.32	0.24
7	0.58	0.73	0.47	0.36	0.72	1.53	1.74	1.87	1.05	0.54	0.45	0.33
8	0.57	0.24	0.24	0.40	0.20	0.00	0.00	0.00	0.00	0.00	0.16	0.34
9	0.85	39.75	39.86	40.09	0.13	57.41	57.08	54.82	39.36	39.68	39.28	19.77
10	8.43	0.46	0.43	0.29	0.18	0.22	0.19	0.17	0.36	0.39	0.70	20.78
11	4.88	0.15	0.05	0.08	10.84	0.05	0.00	0.00	0.00	0.00	0.16	0.17
12	0.31	0.00	0.00	0.00	0.72	0.00	0.00	0.00	0.00	0.00	0.00	0.00
13	99.48	100.25	99.82	99.93	100.00	100.44	100.81	98.60	101.52	100.91	100.83	100.31

	61	62	63	64	65	66	67	68	69	70	71	72
1	238	238	244	244	244	244	244	244	244	244	100	100
2	Di	Gl	Ol	Di	Di	Di	En	En	En	Gl	Ol	Ol
3	53.15	69.75	41.29	52.93	53.87	51.87	57.75	57.48	57.83	55.50	40.99	39.94
4	1.36	0.06	0.07	0.79	0.71	0.89	0.12	0.00	0.11	0.24	0.00	0.00
5	3.57	19.68	0.09	4.98	3.28	4.66	0.44	1.02	0.51	19.28	0.01	0.00
6	0.14	0.02	0.26	0.35	0.30	0.29	0.37	0.38	0.27	0.17	0.47	0.39
7	0.19	0.00	1.12	0.35	0.61	0.67	0.61	0.52	0.63	0.87	2.96	3.60
8	0.21	0.11	0.38	0.59	1.15	0.75	0.44	0.68	0.49	0.48	0.00	0.13
9	19.87	0.08	57.48	20.19	23.00	20.52	39.94	37.95	39.18	11.88	56.15	55.12
10	20.93	0.16	0.27	20.99	17.41	20.23	0.34	0.47	0.57	7.64	0.04	0.19
11	0.26	8.39	0.04	0.26	0.20	0.28	0.07	0.05	0.05	4.39	0.00	0.08
12	0.03	3.01	0.00	0.00	0.04	0.04	0.00	0.00	0.00	0.49	0.00	0.00
13	99.71	101.26	101.00	101.43	100.57	100.20	100.08	98.55	99.64	100.94	100.62	99.45

	73	74	75	76	77	78	79	80	81	82	83	84
1	100	100	100	100	100	100	100	100	100	100	100	100
2	Ol	Ol	Ol	Ol	En	En	En	En	Di	Di	Silica	Silica
3	40.43	58.94	41.75	41.94	58.37	58.67	57.41	57.11	49.90	50.30	100.31	100.35
4	0.06	0.04	0.00	0.04	0.04	0.03	0.00	0.03	1.16	1.01	0.08	0.08
5	0.02	0.07	0.00	0.00	0.16	0.24	0.24	0.18	5.87	6.26	0.11	0.13
6	0.57	0.63	0.41	0.55	0.53	0.62	0.66	0.46	3.36	3.38	0.00	0.00
7	3.30	2.70	1.84	3.06	2.42	2.01	2.14	3.33	2.53	2.63	0.00	0.20
8	0.00	0.00	0.00	0.11	0.18	0.06	0.16	0.21	0.16	0.18	0.00	0.00
9	55.20	37.60	56.05	55.39	37.97	39.26	38.71	38.70	16.34	17.41	0.00	0.00
10	0.07	0.08	0.07	0.11	0.18	0.05	0.28	0.21	20.08	19.42	0.00	0.11
11	0.03	0.00	0.00	0.00	0.00	0.00	0.16	0.05	0.04	0.10	0.00	0.04
12	0.04	0.00	0.00	0.00	0.00	0.00	0.00	0.02	0.00	0.00	0.00	0.04
13	99.72	100.06	100.12	101.20	99.85	100.94	99.76	100.30	99.44	100.69	100.50	100.95

	85	86	87	88	89	90	91	92	93	94	95	96
1	100	100	100	101	101	101	101	101	101	102	102	102
2	Silica	Gl	Gl	En	En	En	Di	Silica	Silica	En	En	En
3	99.29	59.35	60.18	58.17	58.33	59.60	54.32	97.58	99.64	57.43	57.51	56.65
4	0.10	0.56	0.48	0.00	0.07	0.00	0.55	0.00	0.00	0.00	0.00	0.00
5	0.20	23.38	22.89	0.18	0.31	0.18	2.03	1.38	0.57	0.11	0.14	0.11
6	0.00	0.12	0.22	0.76	0.80	0.66	1.46	0.00	0.04	0.94	0.90	0.93
7	0.10	1.93	0.89	2.04	1.93	2.24	1.59	0.12	0.00	4.71	4.34	4.32
8	0.09	0.00	0.00	0.22	0.36	0.10	0.51	0.00	0.00	0.21	0.24	0.07
9	0.00	2.64	2.57	38.98	38.52	37.12	22.52	0.36	0.08	37.10	37.11	36.48
10	0.00	7.65	6.95	0.16	0.24	0.31	16.71	0.30	0.09	0.13	0.11	0.20
11	0.04	5.04	5.23	0.02	0.06	0.00	0.17	0.86	0.36	0.00	0.00	0.05
12	0.03	0.23	0.40	0.00	0.00	0.00	0.02	0.00	0.07	0.00	0.00	0.00
13	99.85	100.90	99.81	100.53	100.62	100.21	99.88	100.60	100.85	100.63	100.35	98.81

	97	98	99	100	101	102	103	104	105	106	107	108
1	116	116	116	124	124	124	124	124	124	124	126	126
2	En	En	En	Ol	Ol	Ol	Ol	En	Di	dGl	En	En
3	57.70	57.61	57.96	40.53	40.70	40.91	40.76	57.06	54.37	92.97	57.79	58.62
4	0.00	0.12	0.00	0.04	0.05	0.09	0.09	0.10	1.25	0.12	0.00	0.02
5	0.21	0.14	0.20	0.00	0.00	0.00	0.00	0.21	5.32	1.48	0.17	0.31
6	1.29	1.22	1.12	0.40	0.38	0.37	0.30	0.48	0.21	0.04	0.55	0.48
7	4.51	5.19	4.47	1.06	1.44	1.56	1.40	0.92	0.00	0.15	1.33	1.09
8	0.15	0.21	0.21	0.21	0.00	0.21	0.21	0.38	0.32	0.00	0.25	0.06
9	36.54	36.25	37.04	56.15	57.46	56.83	56.30	39.06	20.59	1.68	39.00	37.81
10	0.21	0.13	0.16	0.06	0.00	0.04	0.05	0.31	16.36	0.41	0.26	0.48
11	0.13	0.08	0.05	0.08	0.00	0.00	0.00	0.13	1.27	0.64	0.09	0.10
12	0.00	0.03	0.04	0.00	0.00	0.00	0.00	0.00	0.09	0.10	0.00	0.03
13	100.74	100.98	101.25	98.53	100.03	100.01	99.11	98.65	99.78	97.59	99.44	99.00

	109	110	111	112	113	114	115	116	117	118	119	120
1	126	126	126	127	127	127	127	127	128	128	128	128
2	Silica	Silica	Silica	En	En	En	Di	dGl	En	En	Silica	Ab
3	97.91	97.86	98.92	57.77	57.55	57.12	51.73	96.47	58.31	58.83	98.47	67.85
4	0.00	0.05	0.00	0.11	0.06	0.08	1.87	0.06	0.00	0.00	0.00	0.00
5	0.29	0.38	0.26	0.26	0.15	0.35	6.40	1.48	0.16	0.14	0.16	20.51
6	0.00	0.05	0.00	0.50	0.57	0.44	0.27	0.00	0.33	0.40	0.00	0.07
7	0.12	0.00	0.00	0.70	0.67	0.81	0.79	0.22	0.84	1.21	0.23	0.81
8	0.00	0.00	0.00	0.00	0.14	0.10	0.14	0.00	0.00	0.00	0.12	0.00
9	0.26	0.15	0.17	39.38	39.30	39.44	18.63	0.59	39.24	39.75	0.09	0.35
10	0.17	0.81	0.00	0.26	0.29	0.51	19.12	0.30	0.18	0.19	0.00	0.00
11	0.28	0.31	0.18	0.10	0.08	0.12	0.78	0.98	0.05	0.00	0.12	11.29
12	0.00	0.00	0.00	0.00	0.00	0.00	0.15	0.00	0.00	0.00	0.00	0.00
13	99.03	99.61	99.53	99.08	98.81	98.97	99.88	100.10	99.11	100.52	99.19	100.88

	121	122	123	124	125	126	127	128	129	130	131	132
1	137	137	137	137	154	154	154	154	154	154	154	154
2	En	En	En	Silica	Br	Br	Br	Br	Br	Br	Br	Br
3	57.51	57.09	58.55	98.85	56.10	55.59	56.66	55.51	55.33	55.23	55.24	54.33
4	0.08	0.05	0.12	0.07	0.00	0.00	0.00	0.00	0.00	0.04	0.00	0.05
5	0.19	0.17	0.20	0.72	0.15	0.06	0.10	0.48	0.30	0.29	0.37	0.26
6	0.47	0.43	0.44	0.02	1.28	1.12	1.62	1.69	1.64	1.91	1.82	1.96
7	0.82	0.72	0.54	0.00	6.52	7.87	10.21	11.01	11.55	12.23	12.64	13.16
8	0.00	0.13	0.14	0.05	0.00	0.06	0.16	0.00	0.29	0.13	0.09	0.21
9	40.17	39.91	39.94	0.27	34.90	34.40	31.49	31.26	29.98	30.08	29.08	28.89
10	0.40	0.28	0.26	0.10	0.05	0.08	0.06	0.53	0.66	0.34	0.44	0.29
11	0.09	0.00	0.14	0.55	0.00	0.00	0.03	0.03	0.00	0.03	0.00	0.04
12	0.00	0.00	0.00	0.00	0.00	0.04	0.00	0.00	0.02	0.05	0.00	0.00
13	99.73	98.78	100.33	100.63	99.00	99.22	100.33	100.51	99.77	100.33	99.68	99.19

	133	134	135	136	137	138	139	140	141	142	143	144
1	154	154	154	154	154	154	154	154	154	154	161	161
2	Br	Br	Br	Br	Br	Br	Br	Br	rim Qz	rim Qz	En	En
3	54.94	54.53	55.96	55.09	56.71	56.71	52.43	55.37	99.06	98.45	59.75	58.71
4	0.03	0.00	0.07	0.00	0.00	0.02	0.09	0.00	0.00	0.00	0.00	0.07
5	0.25	0.28	0.44	0.24	0.10	0.20	0.21	0.25	0.00	0.03	0.28	0.30
6	1.91	1.95	1.72	1.59	1.14	1.22	2.06	1.55	0.01	0.06	0.88	0.83
7	15.01	15.01	10.08	12.76	7.41	6.86	17.16	11.26	0.30	0.43	2.05	2.05
8	0.14	0.12	0.11	0.17	0.11	0.00	0.14	0.12	0.00	0.00	0.00	0.00
9	28.73	28.01	32.28	30.05	34.17	34.88	28.11	31.22	0.03	0.08	38.35	38.84
10	0.34	0.25	0.47	0.32	0.04	0.10	0.32	0.30	0.03	0.00	0.28	0.23
11	0.00	0.11	0.03	0.00	0.04	0.00	0.03	0.02	0.00	0.00	0.00	0.04
12	0.02	0.00	0.00	0.00	0.00	0.04	0.00	0.02	0.00	0.00	0.00	0.03
13	101.37	100.26	101.16	100.22	99.72	100.03	100.55	100.11	99.43	99.05	101.59	101.10

	145	146	147	148	149	150	151	152	153	154	155	156
1	161	161	161	161	161	161	161	161	175	175	175	175
2	En	Di	Di	Silica	Silica	Silica	Silica	Gl	En	En	En	En
3	58.63	53.86	54.10	100.15	99.92	98.92	100.30	65.25	59.50	58.72	58.33	58.62
4	0.08	0.64	0.35	0.00	0.00	0.03	0.00	0.41	0.00	0.06	0.06	0.05
5	0.40	2.70	2.02	0.11	0.09	0.10	0.09	21.05	0.14	0.28	0.23	0.08
6	0.67	1.58	1.50	0.00	0.02	0.04	0.00	0.14	0.55	0.41	0.34	0.32
7	1.70	1.52	1.69	0.00	0.00	0.00	0.00	0.86	1.02	1.02	0.41	0.64
8	0.15	0.21	0.39	0.00	0.00	0.00	0.00	0.00	0.17	0.00	0.00	0.14
9	38.92	24.09	23.90	0.23	0.14	0.09	0.13	0.18	38.41	38.41	40.13	39.61
10	0.24	15.45	16.06	0.04	0.00	0.00	0.06	0.19	0.36	0.43	0.45	0.25
11	0.08	0.32	0.09	0.11	0.13	0.13	0.04	8.76	0.04	0.00	0.00	0.05
12	0.04	0.00	0.00	0.00	0.00	0.00	0.00	1.71	0.00	0.00	0.00	0.00
13	100.91	100.37	100.10	100.64	100.30	99.31	100.62	98.55	100.19	99.33	99.95	99.76

	157	158	159	160	161	162	163	164	165	166	167	168
1	175	175	268	268	268	268	268	268	268	268	307	307
2	En	Silica	En	En	En	En	En	Di	Di	Gl	Ol	Ol
3	58.78	98.38	60.03	59.43	59.09	58.45	57.90	52.53	51.55	70.20	41.27	41.71
4	0.08	0.06	0.00	0.07	0.07	0.12	0.00	1.20	1.48	0.05	0.00	0.02
5	0.10	0.88	0.18	0.18	0.24	0.31	0.41	4.88	5.07	19.41	0.00	0.00
6	0.43	0.00	0.40	0.39	0.37	0.42	0.36	0.29	0.38	0.00	0.45	0.52
7	1.03	0.00	0.73	0.75	0.47	1.07	0.28	0.17	0.13	0.00	2.33	2.06
8	0.00	0.00	0.20	0.00	0.30	0.13	0.36	0.36	0.22	0.00	0.27	0.21
9	39.92	0.21	38.41	39.07	40.08	39.56	40.06	19.94	19.59	0.24	54.98	55.52
10	0.28	0.05	0.19	0.12	0.37	0.22	0.43	21.63	20.60	0.12	0.04	0.17
11	0.00	0.46	0.11	0.07	0.11	0.00	0.05	0.15	0.21	9.63	0.00	0.00
12	0.00	0.04	0.00	0.00	0.00	0.00	0.03	0.00	0.06	0.46	0.00	0.00
13	100.62	100.08	100.25	100.08	101.10	100.28	99.88	101.15	99.29	100.11	99.34	100.21

	169	170	171	172	173	174	175	176	177	178	179	180
1	307	307	307	307	307	307	307	307	307	307	307	307
2	Ol	Ol	Ol	Ol	Ol	En	En	En	En	En	sEn	Silica
3	41.61	41.15	41.37	41.23	41.76	58.43	57.98	58.00	58.70	58.71	58.41	100.54
4	0.05	0.03	0.06	0.00	0.00	0.08	0.00	0.15	0.04	0.08	0.00	0.03
5	0.00	0.00	0.00	0.00	0.00	0.15	0.15	0.57	0.12	0.08	0.00	0.14
6	0.43	0.45	0.31	0.36	0.43	0.64	0.83	0.62	0.90	0.80	0.00	0.00
7	2.25	2.64	1.31	1.40	1.98	1.50	2.14	1.86	1.99	1.96	0.35	0.06
8	0.18	0.18	0.00	0.00	0.00	0.25	0.28	0.12	0.15	0.00	0.00	0.09
9	55.45	55.66	56.41	55.51	55.07	37.87	38.04	37.62	37.58	38.02	41.04	0.02
10	0.07	0.06	0.08	0.14	0.11	0.25	0.27	0.31	0.31	0.32	0.06	0.06
11	0.00	0.00	0.00	0.00	0.00	0.00	0.07	0.00	0.00	0.00	0.00	0.03
12	0.00	0.00	0.00	0.00	0.00	0.00	0.00	0.00	0.00	0.00	0.00	0.00
13	100.04	100.17	99.54	98.64	99.35	99.17	99.76	99.25	99.79	99.97	99.86	100.97

Appendix III

Chemical compositions of the constituents in cryptocrystalline chondrules (Nos. 131, 138, 150, 171, 213, 215, 219, and 221) and a transparent-SiO_2 chondrule (No. 142). Px, MPx, Silica, MSi, Gm, and Core are pyroxene, mantle pyroxene in concentric chondrules, silica mineral, mantle silica-mineral in concentric chondrules, groundmass, and core of concentric chondrules, respectively.

	1	2	3	4	5	6	7	8	9	10	11	12
1		131	131	138	138	150	150	150	150	171	213	213
2		Core	MPx	MSi	MSi	Silica	Silica	Gm	Gm	Gm	Silica	Gm
3	SiO2	49.13	51.32	98.34	98.64	99.88	99.41	55.80	56.50	51.43	99.56	54.67
4	TiO2	0.13	0.26	0.00	0.04	0.00	0.00	0.09	0.12	0.14	0.00	0.10
5	Al2O3	5.02	5.24	0.03	0.06	0.03	0.06	2.23	2.47	1.36	0.02	2.15
6	Cr2O3	0.41	0.33	0.00	0.03	0.06	0.05	0.81	0.75	0.70	0.02	0.75
7	FeO	0.53	0.78	0.56	0.10	0.24	0.21	2.65	2.87	2.69	0.34	10.13
8	MnO	0.13	0.14	0.00	0.00	0.00	0.00	0.31	0.28	0.00	0.00	0.19
9	MgO	39.39	38.24	0.17	0.14	0.00	0.06	35.32	33.98	43.00	0.05	30.24
10	CaO	1.10	3.84	0.07	0.04	0.00	0.00	1.40	1.71	1.15	0.01	1.72
11	Na2O	2.32	0.40	0.00	0.04	0.00	0.07	0.34	0.60	0.11	0.06	0.66
12	K2O	0.25	0.03	0.00	0.00	0.00	0.00	0.08	0.13	0.00	0.00	0.05
13	Total	98.41	100.58	99.17	99.09	100.21	99.86	99.03	99.41	100.58	100.06	100.66

	13	14	15	16	17	18	19
1	213	215	219	219	221	221	142
2	Gm	MSi	Silica	Silica	Silica	Gm	Silica
3	55.06	99.44	98.52	99.17	98.14	56.78	98.02
4	0.14	0.00	0.06	0.18	0.00	0.11	0.05
5	1.52	0.13	0.43	0.70	0.05	2.70	0.03
6	0.76	0.00	0.00	0.00	0.05	0.77	0.13
7	10.46	0.18	0.21	0.00	1.28	4.57	0.70
8	0.26	0.00	0.04	0.00	0.00	0.51	0.00
9	31.28	0.00	0.08	0.14	0.19	31.92	0.36
10	0.73	0.00	0.75	0.18	0.18	2.70	0.00
11	0.15	0.04	0.31	0.35	0.04	0.93	0.00
12	0.00	0.00	0.00	0.00	0.00	0.19	0.00
13	100.36	99.79	100.40	100.72	99.93	101.18	99.29

Appendix IV

Chemical composition (wt%) of troilite (Tr) and Fe-metal (Met) in barred-Ol-Px chondrule No. 169, porphyritic to granular chondrules Nos. 109, 110, 117, 158, and 159, and radial-Px chondrules Nos. 102, 128, and 307.

	169	109	110	117	117	158	158	159	102	128	307
	Tr	Tr	Tr	Tr	Met	Tr	Met	Met	Tr	Tr	Tr
Fe	58.58	61.28	61.18	54.34	96.98	60.46	95.99	94.78	56.01	61.55	61.61
Ni	0.12	0.04		0.20	2.56	0.10	2.32	3.57	0.03	0.08	0.02
Cr	1.29	1.04	1.30	6.78	0.02	1.67	0.10	0.01	5.61	1.22	1.09
Si					1.52		1.99	2.36			
S	37.40	36.18	36.94	37.05		36.24			38.09	36.83	36.50
Total	97.39	98.54	99.42	98.37	101.08	98.47	100.40	100.72	99.74	99.68	99.22